

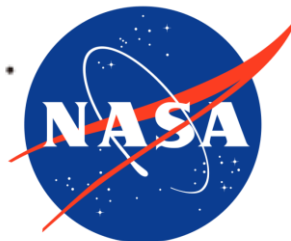
CCN and INP Abilities of Aerosol Particles Measured during HIWC-2022 and CPEX-CV campaigns

*Narihiro ORIKASA¹, Masataka MURAKAMI^{2,1}, Ayumi IWATA¹, Atsushi MATSUKI³,
Masayuki TODA³, and HIWC Science Team (NASA/FAA)

¹ Meteorological Research Institute, Tsukuba, Japan

² Institute for Space-Earth Environmental Research, Nagoya University, Nagoya, Japan

³ Institute of Nature and Environmental Technology, Kanazawa University, Kanazawa, Japan



HIWC-2022 Special Topics Meeting
29-30 Nov. 2023, @NCAR

Outline

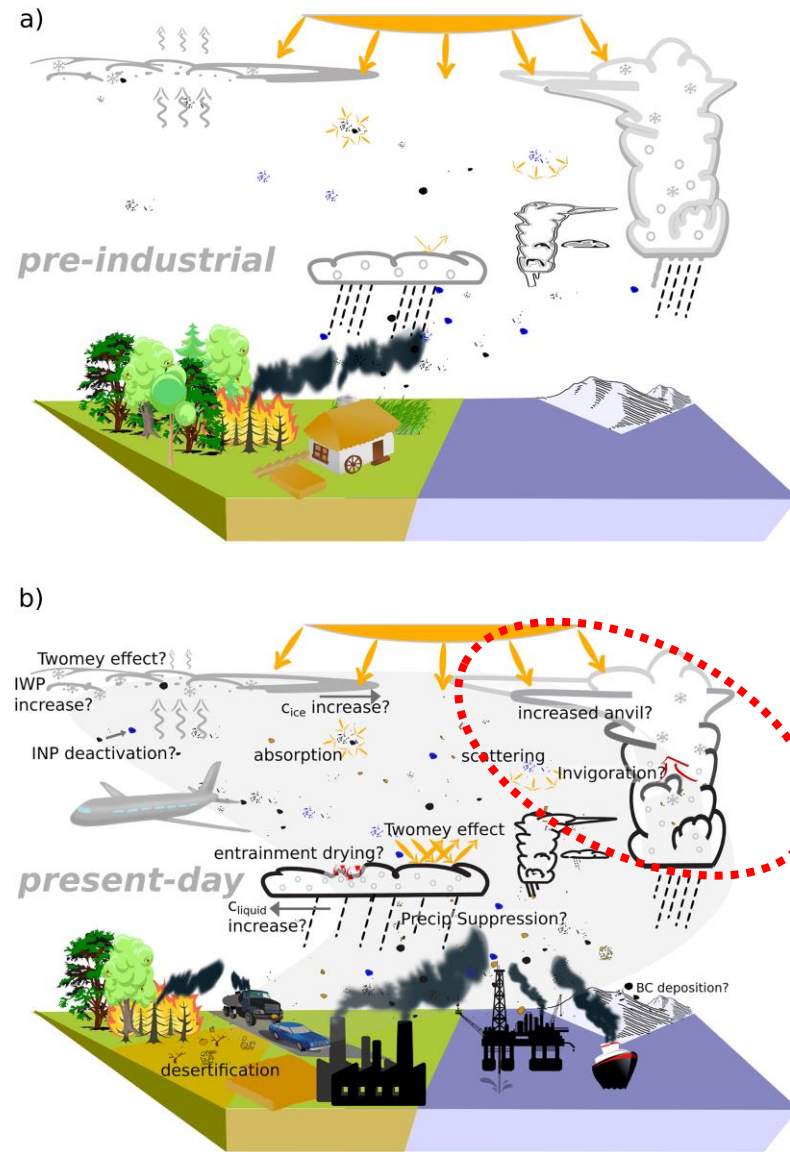
1. Introduction
2. Instrumentation, methods, and data
3. CCN ability and aerosol properties
4. INP ability **(#1)** measured with Raman spectroscopy (by Mr. Toda)
5. INP ability **(#2)** measured with TEM analysis (by Dr. Iwata)
6. Summary

Aerosol-cloud interactions



Fig. 1. Clouds in the presence of anthropogenic haze over the equatorial Indian Ocean. Picture taken on 24 February 1999 at 0.5°N, 73.3°E during the Indian Ocean Experiment campaign. The brownish haze originates from South Asia (see Web fig. 1 for a photo of thick brownish haze over lower Himalayas). The haze reaches close to the top of cumulus clouds located around 5 km in this picture.

Anthropogenic aerosols may alter precipitation patterns and surface temperature structures.
[Ramanathan et al., 2001]



CCN and INPs are important in climate systems via indirect effects on cloud radiative forcing and on precipitation.
[Bellouin et al., 2019]

Figure 2. Simplified representation of the impact of anthropogenic aerosol emissions on the Earth system in (a) the preindustrial and (b) the present-day atmosphere. A schematic representation of known processes relevant for the effective radiative forcing of anthropogenic aerosol is summarized for present-day conditions in panel (b), but the same processes were active, with different strengths, in preindustrial conditions. Processes where the impact on the effective radiative forcing remains qualitatively uncertain are followed by a question mark. C_{liquid} and C_{ice} denote liquid and ice cloud fractions, respectively. LWP and IWP stand for liquid and ice water path, respectively. INP stands for ice nucleating particle.

CCN concentrations

Table 2. Summary of the Measurements in Comparison

Authors	Location	CN Conc. N_{CN}, cm^{-3}	CCN Conc. N_{CCN}, cm^{-3}
<i>Kim et al.</i> [2005] <i>Song and Yum</i> [2004]	Gosan Yellow Sea and the South Sea of Korea west coast of the Korean Peninsula	2800–5600 1000 (maritime), 2000 (continental) 5000	2400–5300 at 1% S 800–2000 at 0.3% S 176 at 1% S
<i>Yum et al.</i> [2005] <i>Adhikari et al.</i> [2005]	west coast of Korean Peninsula remote southwest island of Japan		
<i>Hudson and Yum</i> [2002] <i>Hoppel and Frick</i> [1990] <i>Roberts et al.</i> [2006] <i>Yum and Hudson</i> [2002] <i>Hudson and Yum</i> [2001] <i>Hoppel et al.</i> [1990]	Indian Ocean central Pacific eastern Pacific (pristine-anthropogenic) eastern Pacific <u>off the coast of Florida</u> American Atlantic coast, center of Atlantic, African Atlantic coast, pollution plume in Atlantic	361 150–300 <100–10000 252–325 <u>1200 (maritime), 3600 (continental)</u> 2000, 200, 2000, 10000	20–350 at 0.3% S 112–157 at 0.6% S <u>360 (maritime), 1400 (continental) at 1% S</u>
<i>Yum and Hudson</i> [2002] <i>Chuang et al.</i> [2000] <i>O'Dowd et al.</i> [2001]	eastern Atlantic eastern Atlantic eastern Atlantic coastal site in Mace Head	241–364 400–600 (maritime), 600–1500 (modified maritime air)	126–131 at 0.6% S 27–267 at 0.1% S
<i>Jennings et al.</i> [1998]	eastern Atlantic coastal site in Mace Head		76–203 at 0.5% S (marine air), 369–1428 at 0.5% S (polluted air)
<i>Eleftheriadis et al.</i> [2006] <i>Bates et al.</i> [2000] <i>Yum and Hudson</i> [2004] <i>Yum and Hudson</i> [2001]	coastal site on a remote island in eastern Mediterranean Southern Ocean and northeastern Atlantic Southern Ocean Arctic Ocean	1300 (background), 3400–4000 (polluted) 300–500 260–298 45–497	32–191 at 1% S 41–290 at 0.8% S

Northeast Asia

Pacific

Atlantic

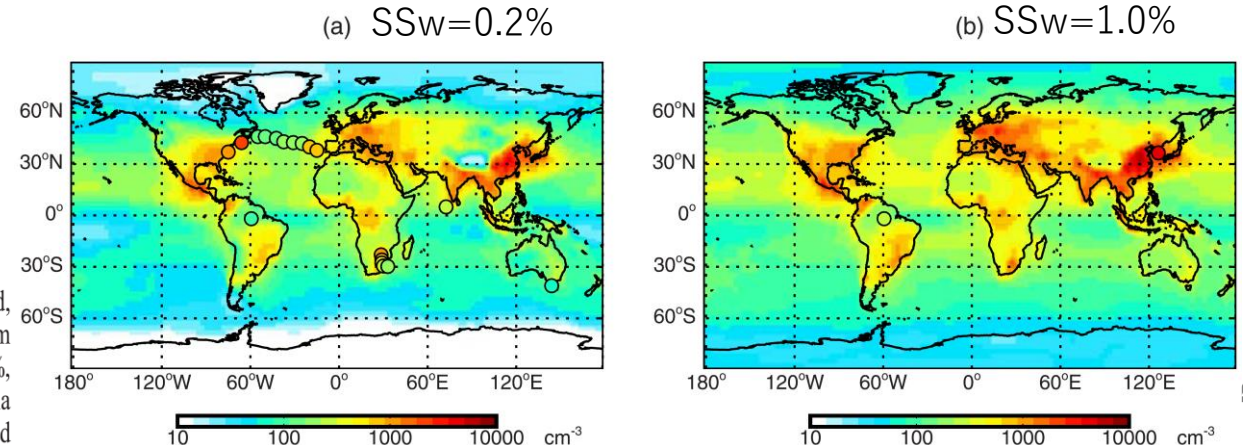
Northeast Asia, polluted in Northern Hemisphere

- CN Conc. : $O(\sim 10^3)$
- CCN Conc. : (High SSw) $O(\sim 10^3)$

Spracklen et al. (2008) GRL

Figure 2. Surface CCN concentrations (cm^{-3}) at (a) 0.2% and (b) 1.0% supersaturation. Model results (background, average for March–May 2000 without BL particle formation) are compared against observations (circles) from Cape Grim (0.23%, March–May) [Ayers et al., 1997], Atlantic Ocean (0.16%, May 1997) [Hoppel, 1979], Indian Ocean (0.23%, February–March 1998) [Cantrell et al., 2000], southern Africa (0.3%, March–April 2001) [Ross et al., 2003], Amazonia (0.3% and 1%, May 1999) [Roberts et al., 2003] and Korea (1%, May 2004) [Yum et al., 2005]. Ratio of simulated

Yum et al. (2007) JGR



Hygroscopicity (κ)

κ - Köhler theory

Petters and Kreidenweis, 2007

$$S = a_w \cdot \exp\left(\frac{4\sigma M_w}{RT\rho_w D}\right)$$

$$\frac{1}{a_w} = 1 + \kappa \frac{V_s}{V_w} \quad \longleftrightarrow \quad \text{Classical Theory} \quad i \frac{M_w m_s}{M_s m_w}$$

$$\kappa = \sum_i \kappa_i \cdot \frac{V_{si}}{V_s}$$

S : saturation ratio
 a_w : water activity
 ρ_w : water density
 M_w : molecular weight of water
 σ : surface tension (solution/air)
 R : universal gas constant
 T : absolute temperature
 D : droplet diameter
 V_w : vol. of water
 V_s : vol. of dry particulate matter
 i : van't Hoff factor
 κ : hygroscopicity parameter

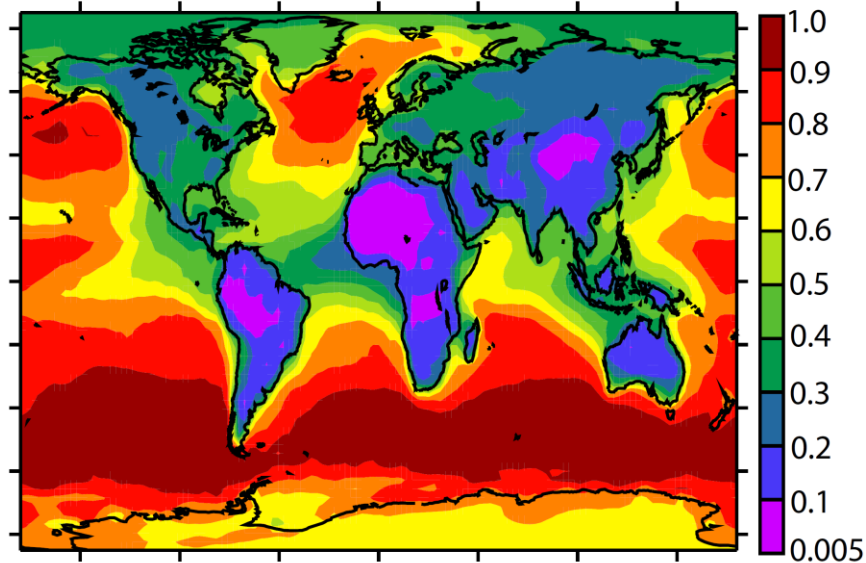


Fig. 1. Annual mean distribution of κ at the surface simulated by EMAC.

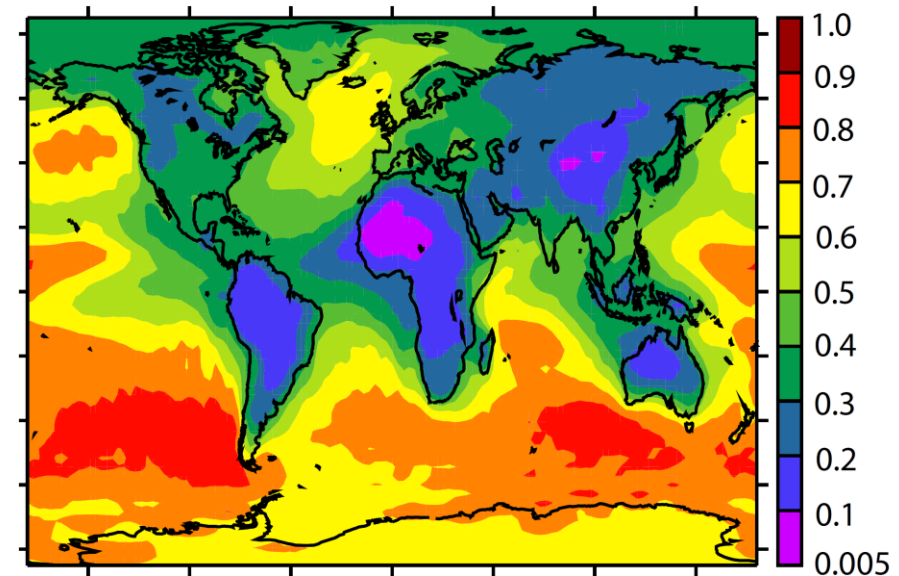


Fig. 2. Annual mean distribution of κ at the altitude of the planetary boundary layer.

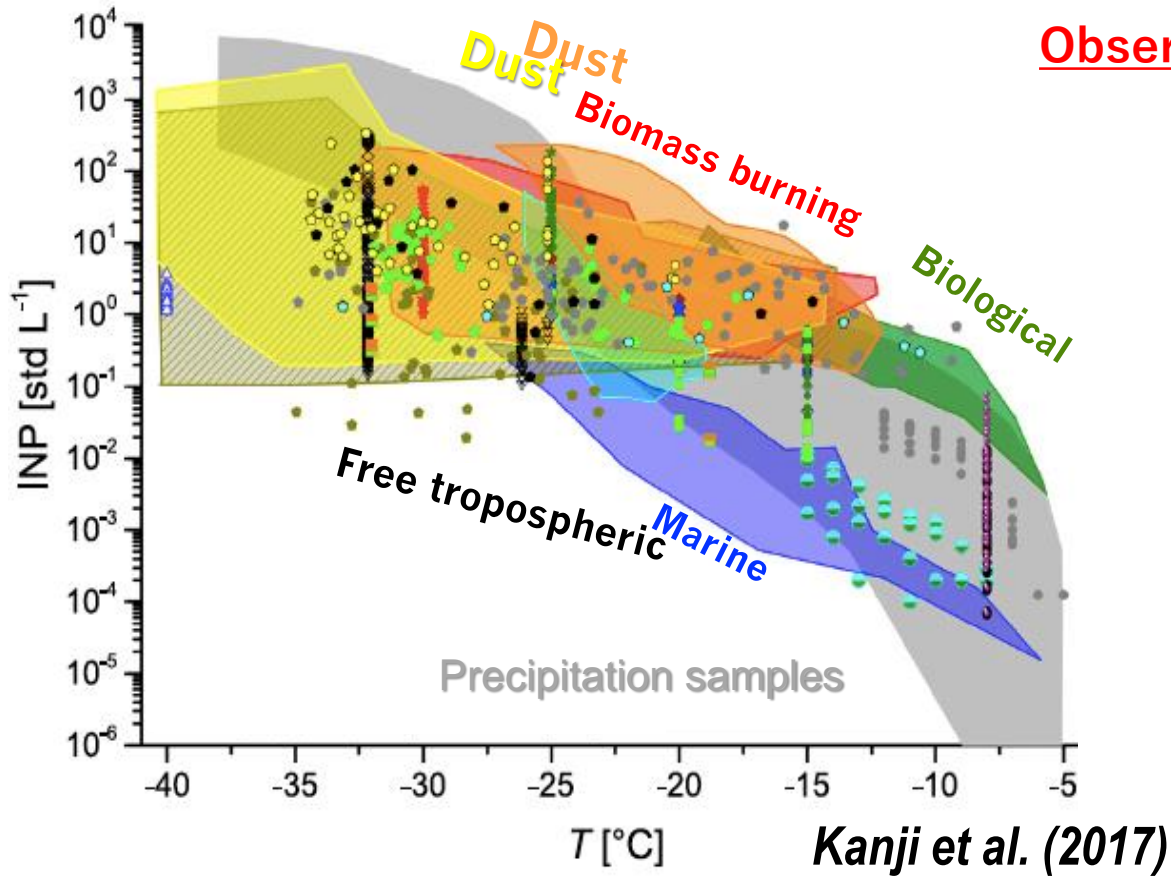
Table 1. Simulated global and regional annual mean κ values (and standard deviation (St Dev)) at the surface and at the simulated PBL height under present day conditions. Standard deviation is calculated for the year from 5-hourly average data. S_c is the critical supersaturation, calculated using the regional mean κ at PBL height. Area column gives total land area for land sites, and marine area for marine sites.

Region	Area (10^{13} m^2)	Mean κ Surface	St Dev Surface	Mean κ PBL height	St Dev PBL height	S_c (%) $D_p=60$ (nm)	S_c (%) $D_p=120$ (nm)
Global (Continental)	14.4	0.27	0.21	0.27	0.20	0.48	0.17
Global (Marine)	37.0	0.72	0.24	0.60	0.25	0.33	0.11
N. America	1.61	0.30	0.15	0.29	0.14	0.47	0.17
S. America	1.90	0.17	0.14	0.18	0.13	0.59	0.21
Africa	3.48	0.15	0.12	0.17	0.11	0.61	0.22
Europe	1.14	0.36	0.16	0.33	0.15	0.44	0.15
Asia	3.64	0.22	0.15	0.22	0.13	0.54	0.19
Australia	0.87	0.21	0.16	0.23	0.15	0.52	0.19
N. Atlantic	1.25	0.59	0.18	0.47	0.18	0.37	0.13
Southern Ocean	1.56	0.92	0.09	0.80	0.17	0.28	0.10

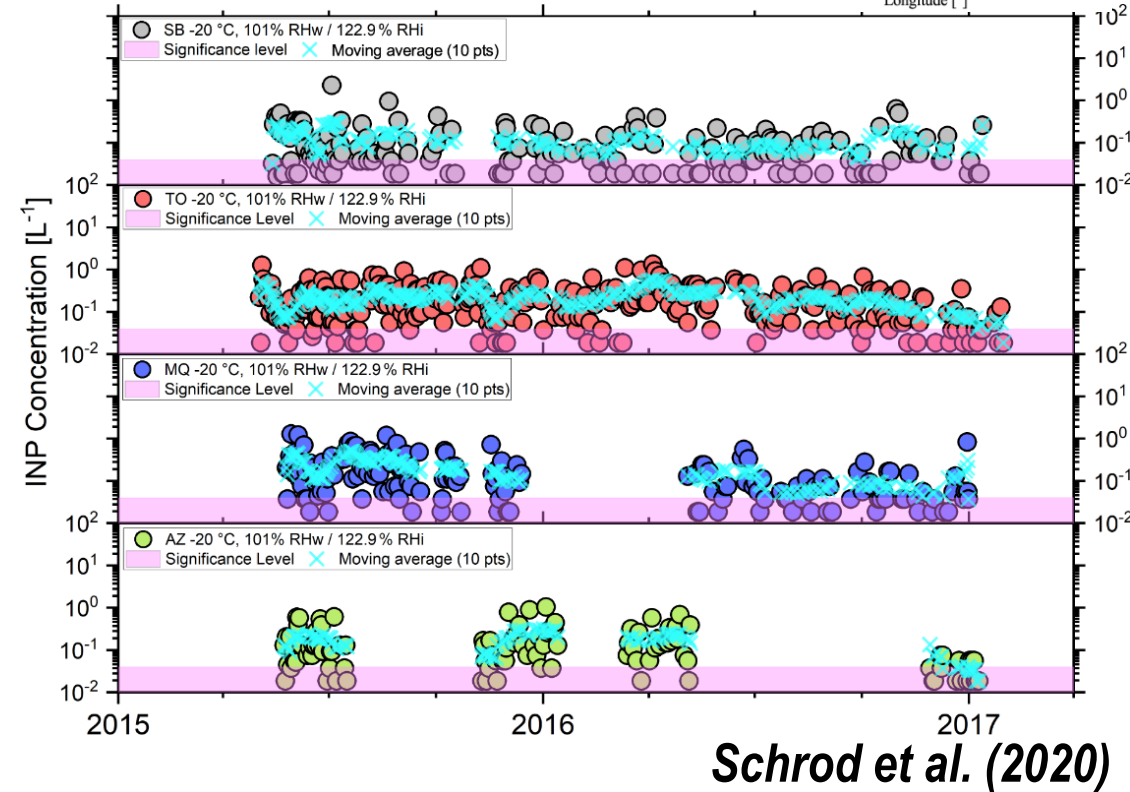
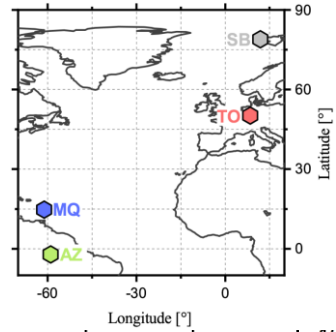
- Evaluated by simulations, but sparse observations.
- Requires more study on size-dependency of CCN ability.

Pringle et al. (2010) *ACR3*

INP concentrations



- More diverse concentrations at any supercooled T in real atmospheric conditions, compared to specific conditions or events.
- Complicated chemical composition and mixing state in real atmospheric conditions.



- Observed INP Conc. do not differ greatly from site to site, in spite of diverse geographical climates, transport patterns, aerosol characteristics, and anthropogenic impacts.
- Short-term variability overwhelms long-term trends and/or seasonality.
- Spatio-temporal distributions of INPs are still poorly understood.

Ice Nucleation Active Surface-site ($INAS; n_s$) density

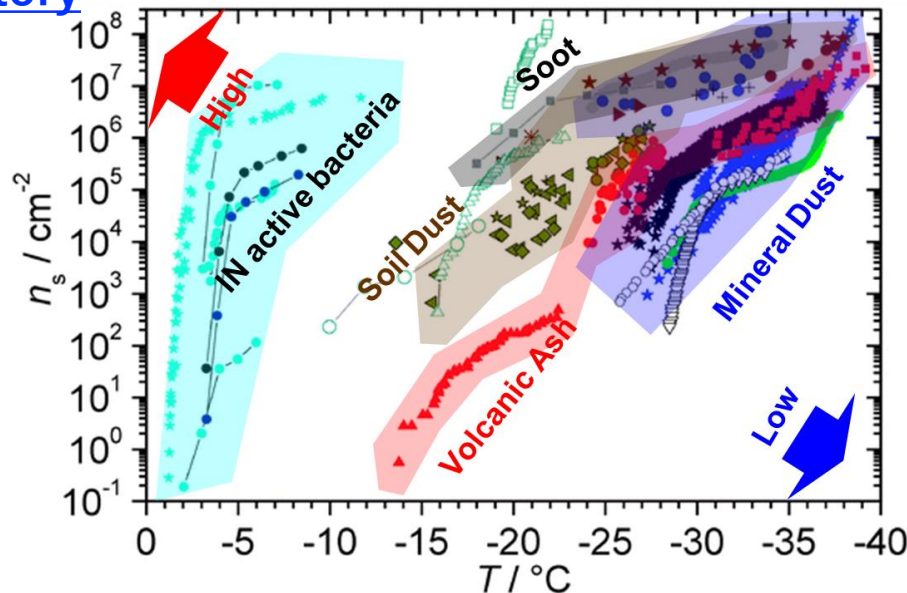
INAS

Connoly et al. 2009; Hoose and Möhler 2012; Kanji et al. 2017; etc.

TABLE 1-1. Definitions of metrics used to summarize and discuss ice nucleation results presented in this chapter.

Metric	Definition
AF Activated Fraction	$AF = N_{ice}/N_{tot}$, where N_{ice} = no. of ice crystals, N_{tot} = total particle no.
F_{ice} Frozen Fraction	$F_{ice} = N_{ice}/(N_{ice} + N_{droplets})$, where $N_{droplets}$ is no. of unfrozen drops
n_s and n_m monodisperse aerosol experiments	$n_s (\# \text{ cm}^{-2}) = -\ln(1 - AF)/A (\text{cm}^2)$; $n_m (\# \text{ mg}^{-1}) = -\ln(1 - AF)/m_{INP} (\text{mg})$; A = surface area of 1 particle m = mass of 1 particle
n_s and n_m approximation for experiments with polydisperse aerosol valid for $AF < 0.1$	$-\ln(1 - AF) \cong AF$; for $AF < 0.1$, $\Rightarrow n_s (\# \text{ cm}^{-2}) = \frac{AF}{A (\text{cm}^2)} = \frac{N_{ice}}{N_{tot} \times A (\text{cm}^2)} = \frac{N_{ice}}{A_{total} (\text{cm}^2)}$ A_{total} = SA of polydisperse size distribution For n_m , A_{total} is replaced with the equivalent mass distribution
Ice onset	Defined variably, ranging from first appearance of ice to AF of 1 Typical values include $AF = 10^{-4}, 10^{-3}, 10^{-2}$, and 10^{-1}

Laboratory



- Various INP ability in each aerosol type.
- Higher INAS in dust and biogenic aerosols.

Murray et al. (2012)

Ice crystal icing (ICI) occurrence

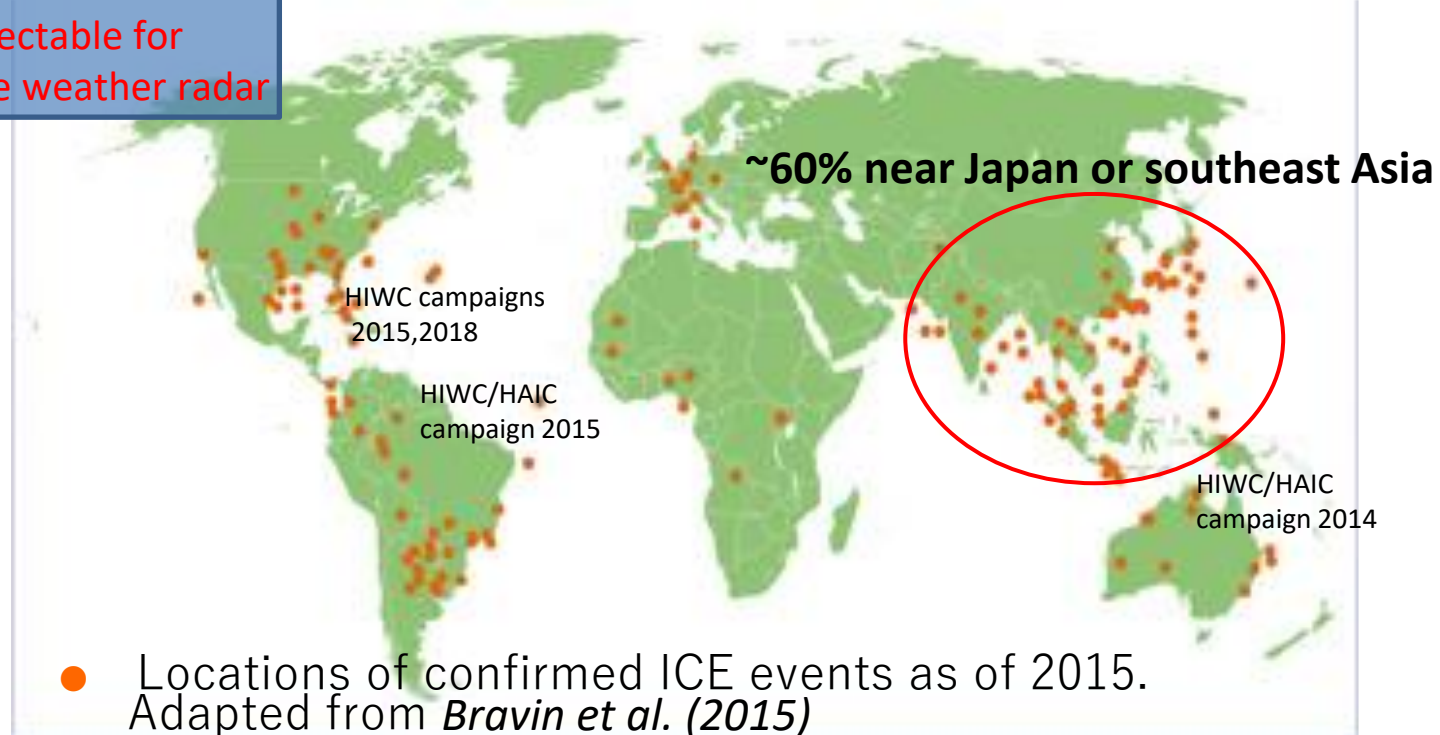
High-level ice clouds sometimes consists of many small ice crystals, which contain high ice water content (HIWC)

Not detectable for airborne weather radar

Pilots **keep flying in those clouds**, not recognizing the aviation hazard of ICI.

Incidents have frequently occurred under such conditions.

Engine icing
Instrument icing



Objectives

(1) HIWC2022 Flight Campaign (2022/Jul/5-Aug/1, FL, USA)

- Understanding of the actual HIWC conditions in [subtropical West Atlantic region](#)
- Investigating of the impact of [high concentrations of aerosols](#) on the HIWC conditions
- Microphysical properties of aerosols and clouds [in towering cumulus and in marine boundary layers](#)

(2) HIWC Supplementary Campaign (CPEX-CV Flight Campaign) (2022/Sep/5-Sep/30, Cabo Verde)

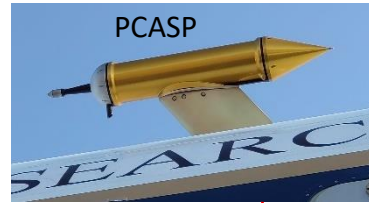
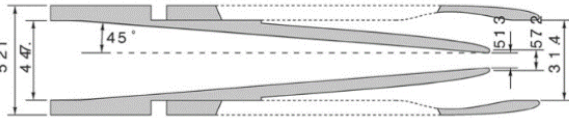
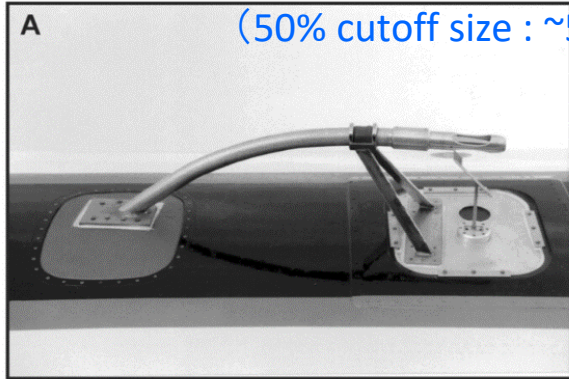
- Understanding of [the interactions between large-scale environmental forcings and lifecycle and properties of convective cloud systems](#) in tropical East Atlantic region
- Assessing the [impact of observations](#) (winds, thermodynamics, clouds, aerosols) [on prediction](#) of tropical weather systems
- [Validation of remote-sensing observations](#) via spaceborne sensors vs airborne ones
- Understanding of the actual HIWC conditions in [tropical East Atlantic region](#)
- Microphysical properties of aerosols and clouds [in high aerosol conditions](#) (Saharan dust layers etc.)

Overview of NASA DC-8 with HIWC-2022 Instrumentation

CPEX-CV

UH Inlet ← *McNaughton et al. 2007*

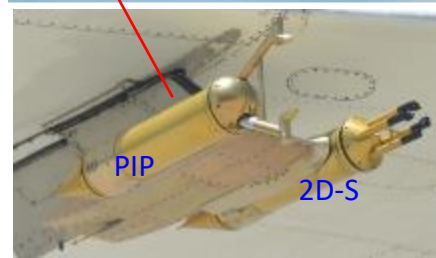
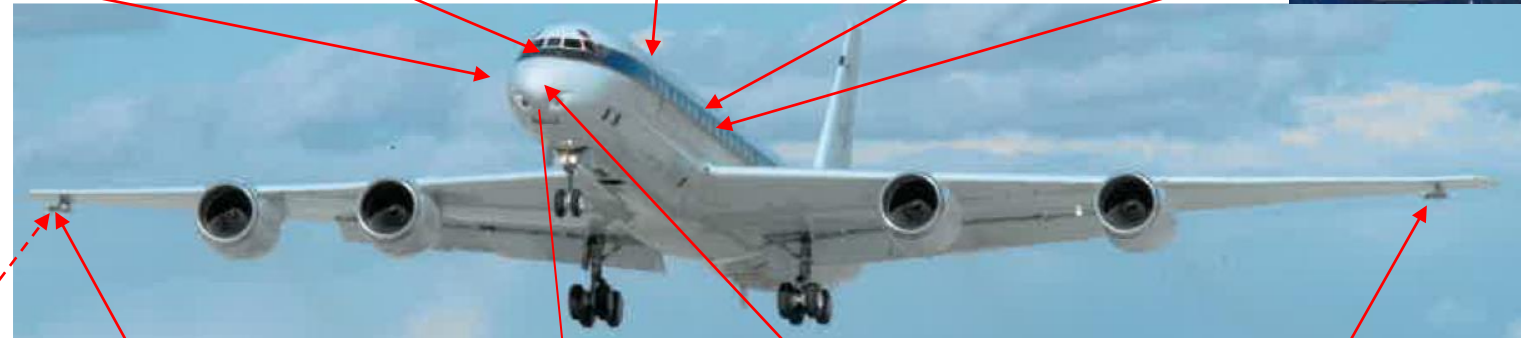
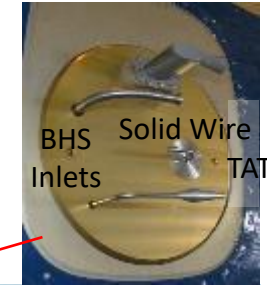
(50% cutoff size : $\sim 5 \mu\text{m}$)



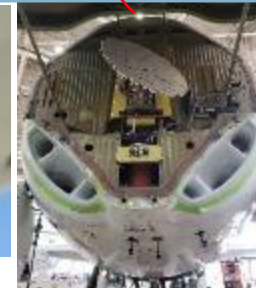
PCASP in SPEC canister on strut at 62° viewport



DLH



MMS Pitot Probe



Modified Honeywell RDR-4000



IKP2

- Cloud particle spectra: CDP-2, 2D-S, PIP, CAPS
- Cloud Water Content: IKP2, SEA TWC/LWC
- RDR-4000 Wx Radar ← *Strapp et al. 2016*
- Diode Laser Hygrometer, Licor/WVSS2 for background water vapor
- UH Inlet and supporting aerosol instrumentation
- Aerosol : PCASP, SMPS(3080+3081), OPC(KC-01E), CCN-200, Impactors(for TEM grid, Silicon Wafer grid), Membrane Filter sampler

Configuration of Aerosol Rack

OPC

Laptop PC for OPC & SMPS

Laptop PC for IN Counter (INC)

Inlet Pressure Control for
CCN Counter (CCNC)

Electrostatic Classifier (EC),
Differential Mobility Analyzer (DMA)



A/D Converter

Membrane Filter (MF) holder sampler

Laptop PC for two Impactors

Impactor#1
(AS-TEM)

Impactor#2
(AS-SW)

Monitor & Keyboard
for M300

M300

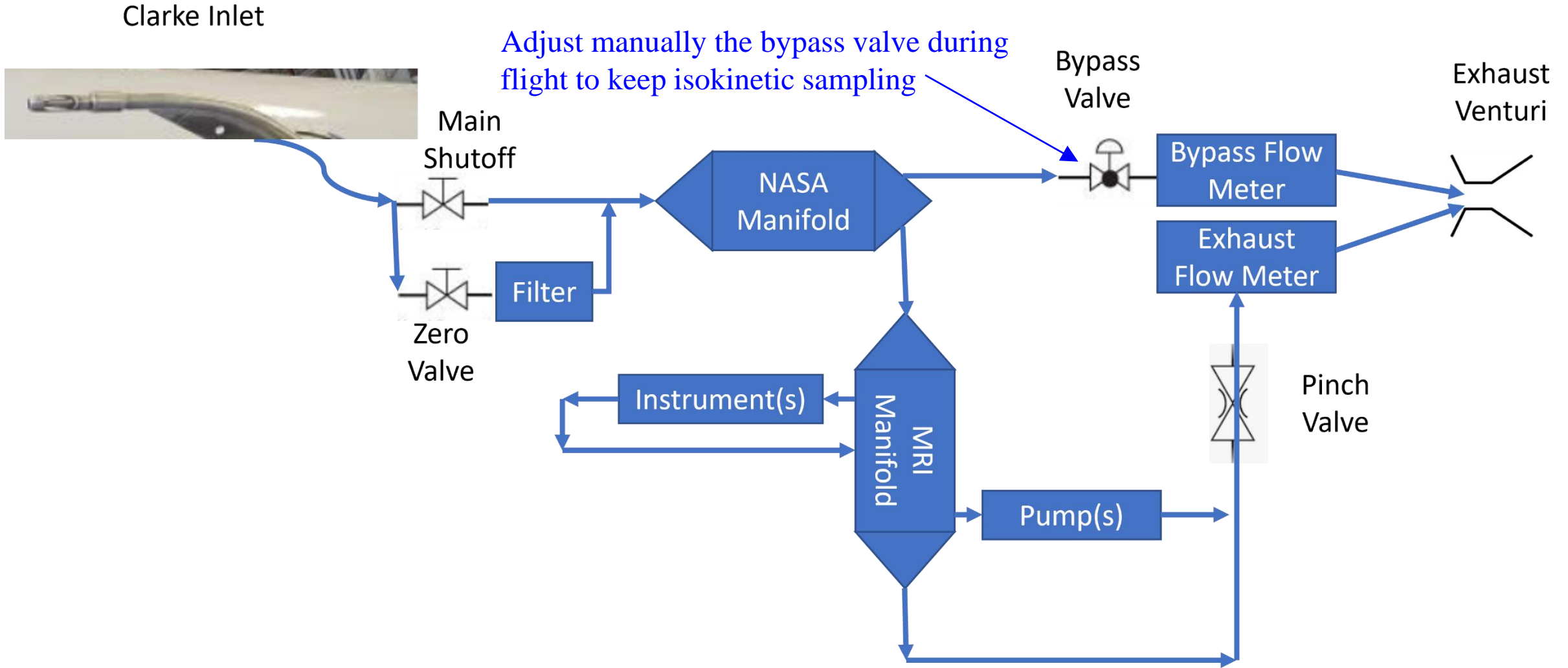
CPC

Bypass valve to keep isokinetic sampling

CCNC Rack

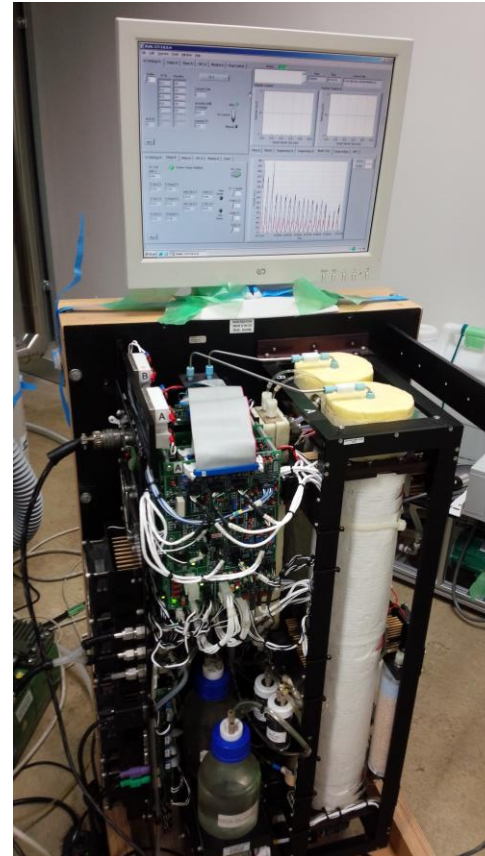
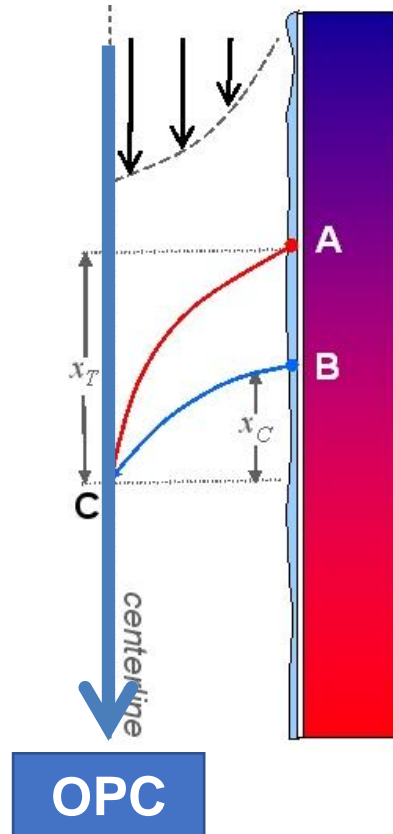


Sampling diagram from inlet to exhaust



CCN counter

(Continuous-Flow Streamwise Thermal-Gradient Chamber)



DMT CCN-200
(dual-column version)

Column-A:
 $SS_w = 0.5\%$ (fix)

Column-B:
 $SS_w = 0.1$ (11), 0.3 (4), 1.0 (5min)%

- water supersaturation in chamber with wetted wall and longitudinal thermal gradient

(Thermal diffusivity $<$ Molecular diffusivity of water vapor)

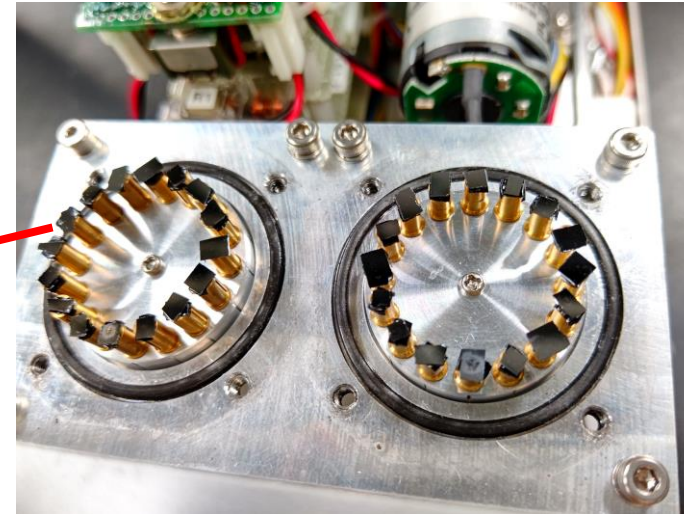
- some aerosols activated to water droplets, counted with OPC

Aerosol Sampling Devices

Impactor sampling (2 types)

TEM grid

cutoff size:
0.7, 0.2 μm

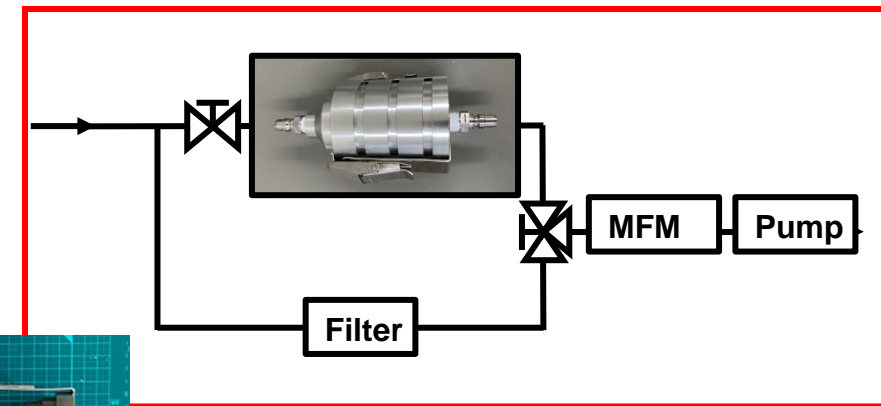
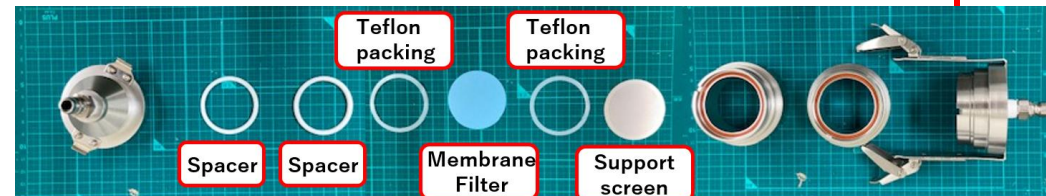


Silicon wafer
cutoff size: 1 μm

Filter sampling

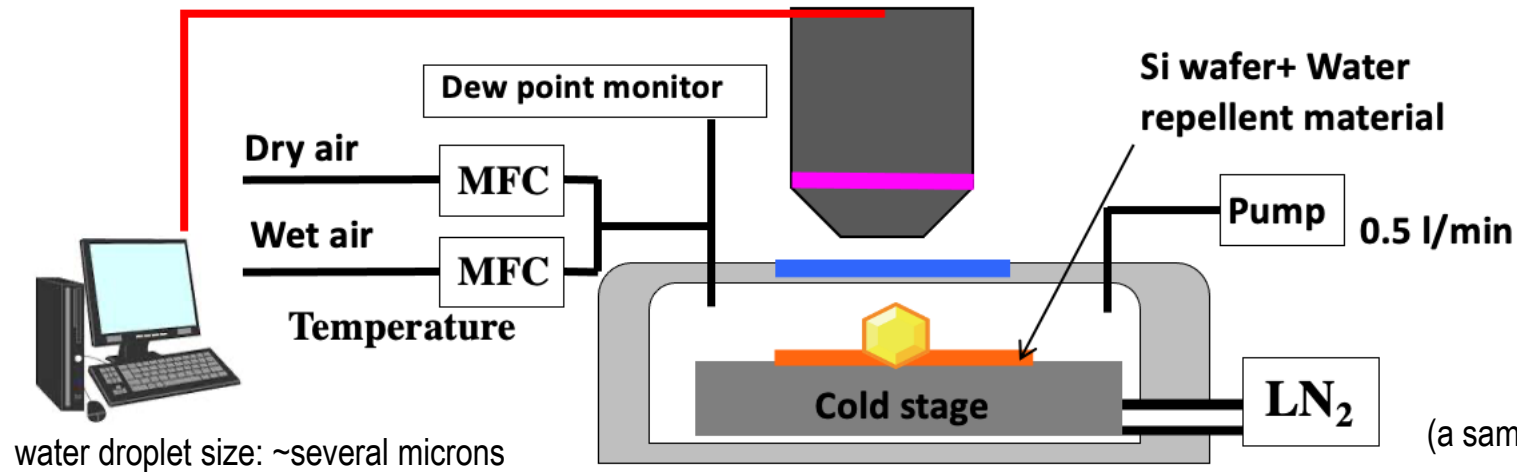


Sartorius PTFE filter
($\phi 47$ mm, pore size 0.45 μm)



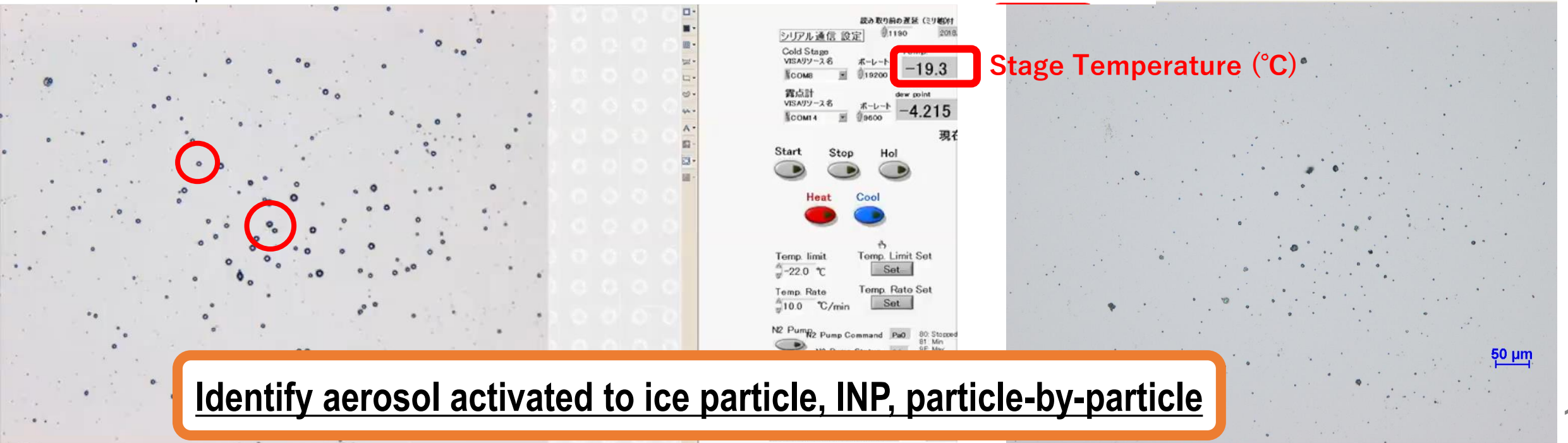
Individual Droplet Freezing Method (IDFM)

Iwata and Matsuki, 2018



water droplet size: ~several microns

(a sample of the same scale as the motion pictures on your left)



Identify aerosol activated to ice particle, INP, particle-by-particle

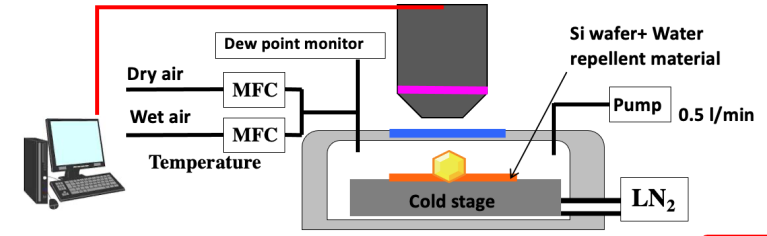
Single INP identification and analysis

IDFM

cooling to -22°C^*

wait 10 sec in case of non-freeze

cooling to -30°C



*ATD freezes at -22°C

Spectrometer systems

INP

Raman : chemical compounds

SEM-EDX : morphology,
elemental composition

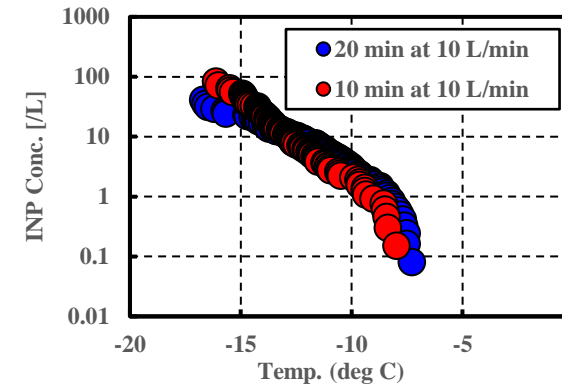
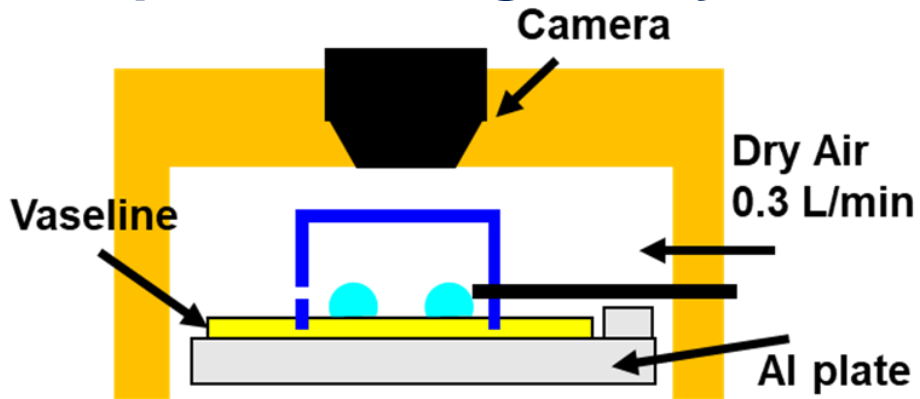


(Nanofinder, Tokyo Instruments)



(JSM-7100F, JEOL)

Droplet Freezing Assay on Filter

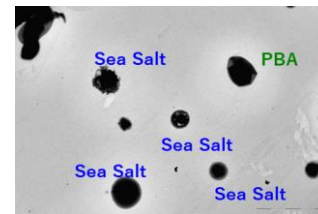


- place an array (~100 #) of ultrapure water droplets (1 μ L) onto PTFE MF
- cooling rate: -1 $^{\circ}$ C/min, record the freezing T for each droplet
- contact angle between MF and droplets: $\alpha=131.6^{\circ}$
- the number of INP in every 0.5 $^{\circ}$ C intervals -> calculate INP conc., INAS

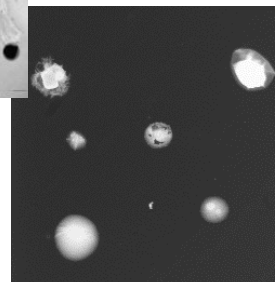
Individual Particle Analysis



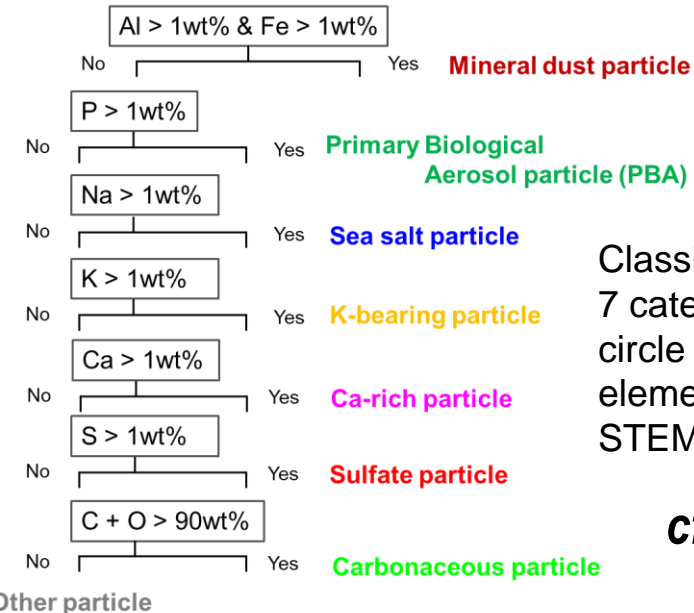
TEM (JEM-1400, JEOL, Tokyo)
+ SEM/EDX (Oxford Inst., Tokyo)



TEM mode



STEM mode



Classify individual particles into 7 categories through equivalent circle diam. by TEM mode and elemental composition by STEM mode (120 kV, 20 sec)

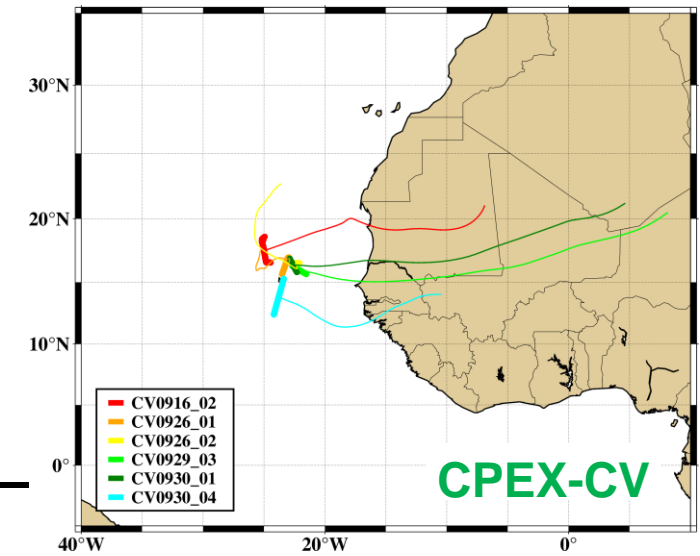
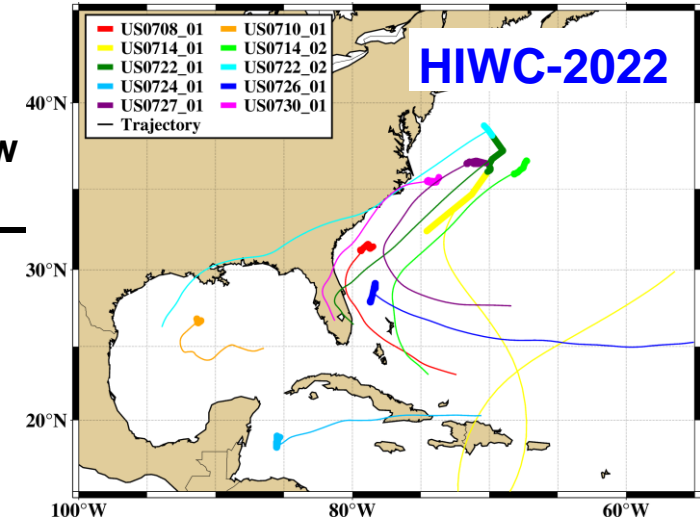
cf. Adachi et al., 2020

Sampling Data (filters)

HIWC-2022
10 samples

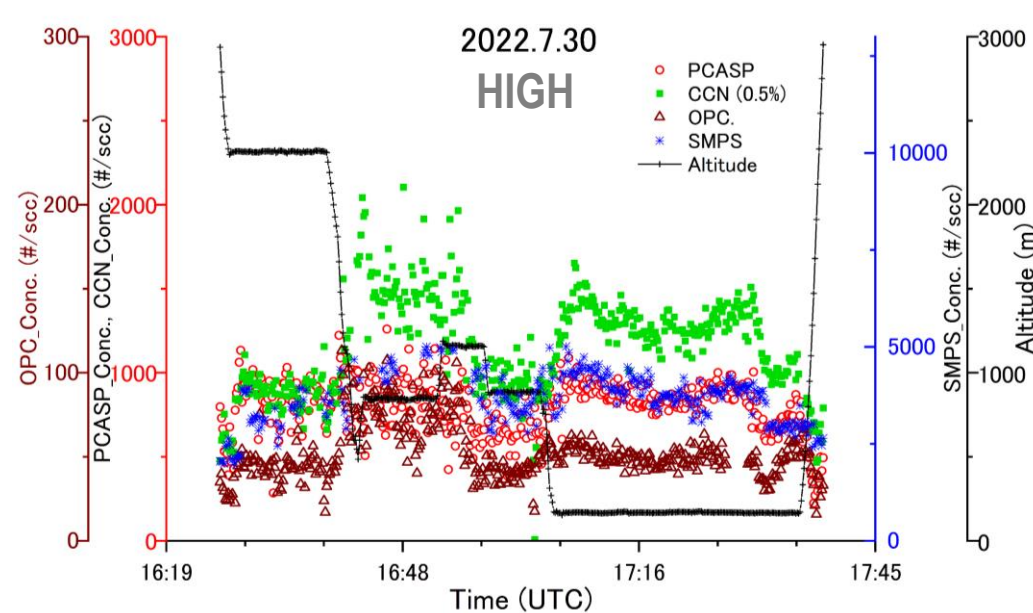
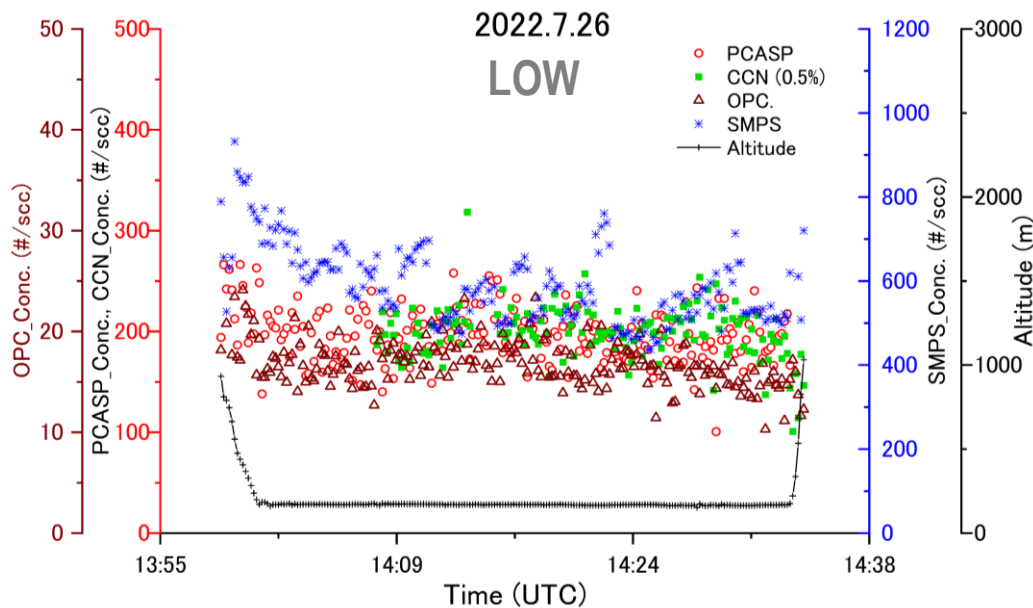
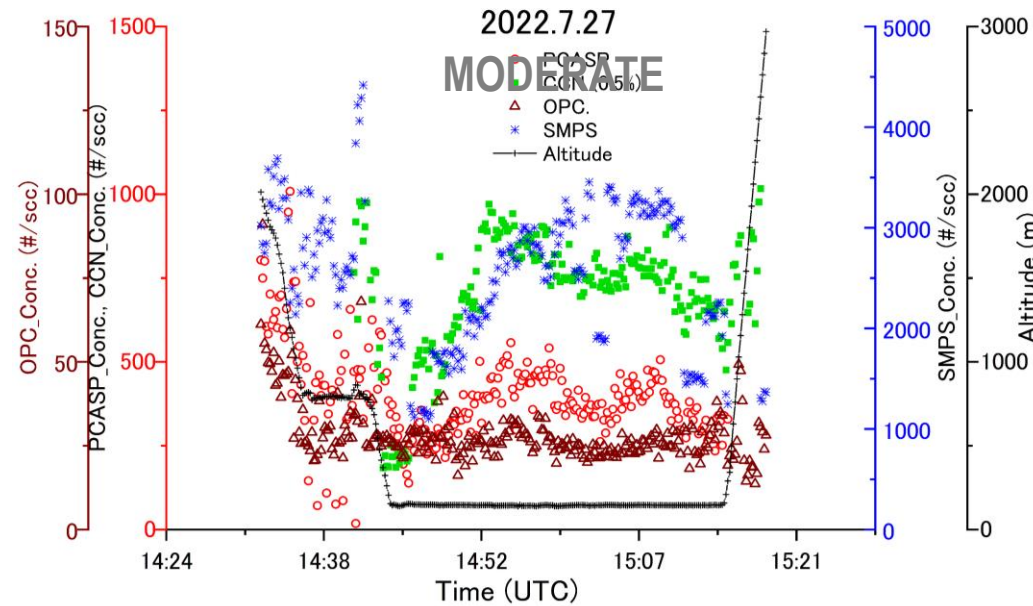
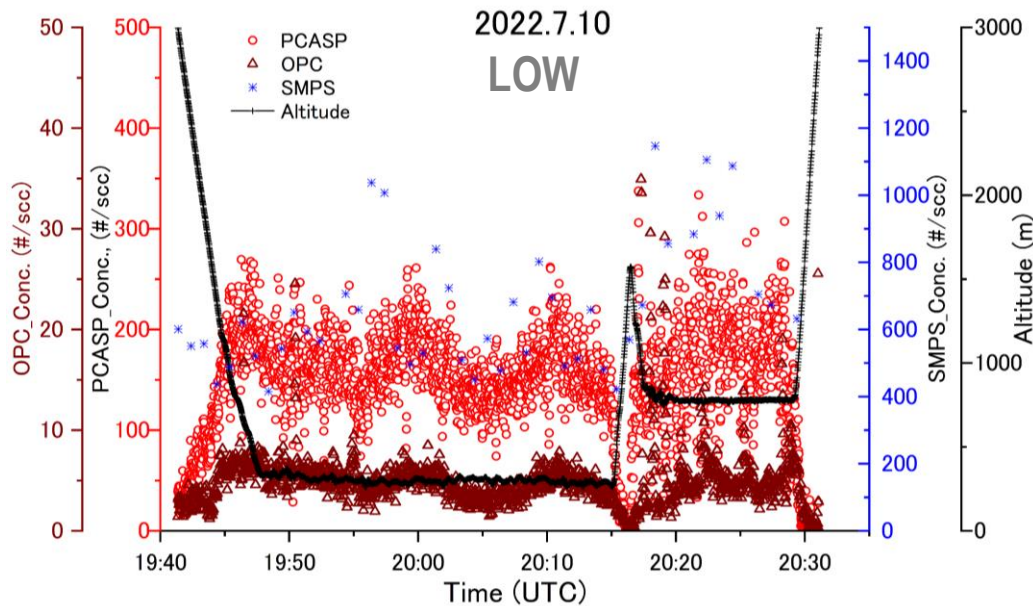
CPEX-CV
6 samples

ID	Date	Start [UTC]	Stop [UTC]	Period [min]	Ave. Alt [m]	Ave. Flow [L/min]
US0708_01	2022/7/8	19:19	19:36	16.8	619.5	12.1
US0710_01	2022/7/10	19:47	20:15	27.3	302.2	18.5
US0714_01	2022/7/14	14:50	15:28	37.8	11012.7	3.8
US0714_02	2022/7/14	17:51	18:16	24.8	340.1	12.1
US0722_01	2022/7/22	13:45	14:21	36.0	186.7	12.4
US0722_02	2022/7/22	14:22	14:33	11.0	190.9	12.6
US0724_01	2022/7/24	14:58	15:28	30.0	189.6	12.1
US0726_01	2022/7/26	14:02	14:33	31.0	169.4	12.4
US0727_01	2022/7/27	14:44	15:14	30.6	146.4	12.7
US0730_01	2022/7/30	17:06	17:36	29.7	168.3	12.5
CV0916_02	2022/9/16	19:51	20:26	35.0	3109.8	7.3
CV0926_01	2022/9/26	5:03	5:19	16.3	5562.1	6.6
CV0926_02	2022/9/26	11:48	11:54	6.3	3185.8	9.6
CV0929_03	2022/9/29	16:09	16:21	11.6	4007.0	8.7
CV0930_01	2022/9/30	8:29	8:41	12.0	5669.4	7.0
CV0930_04	2022/9/30	14:31	14:54	22.9	9389.1	4.6

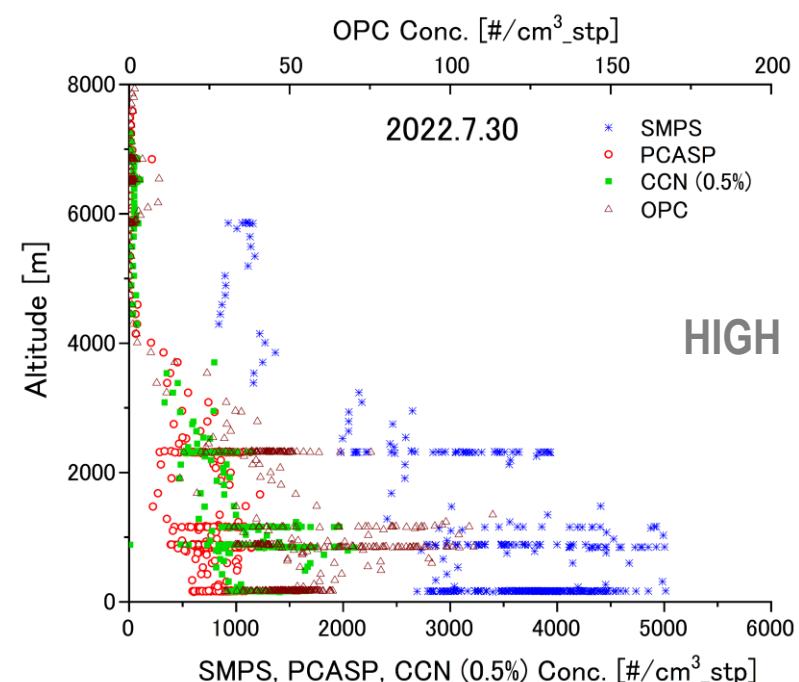
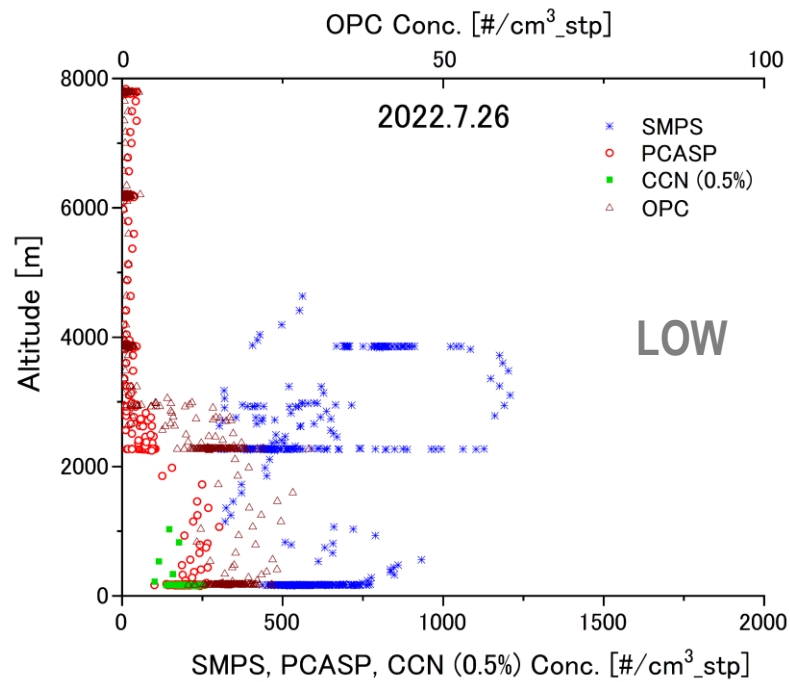
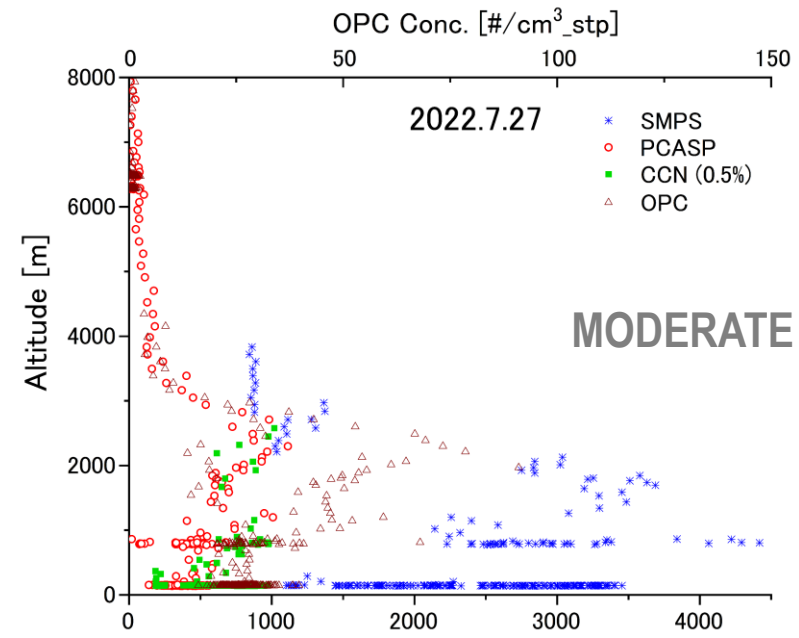
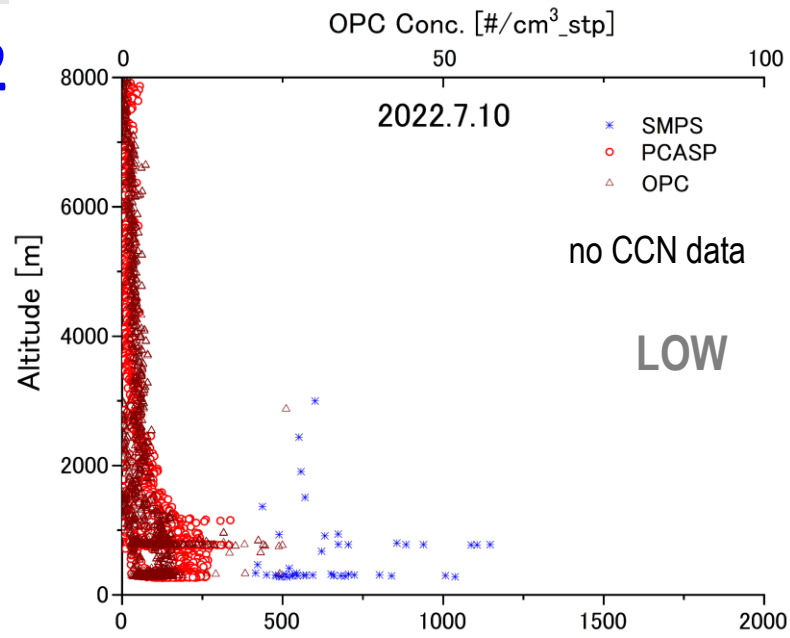


Time series of aerosol conc. (H < 3 km)

HIWC-2022

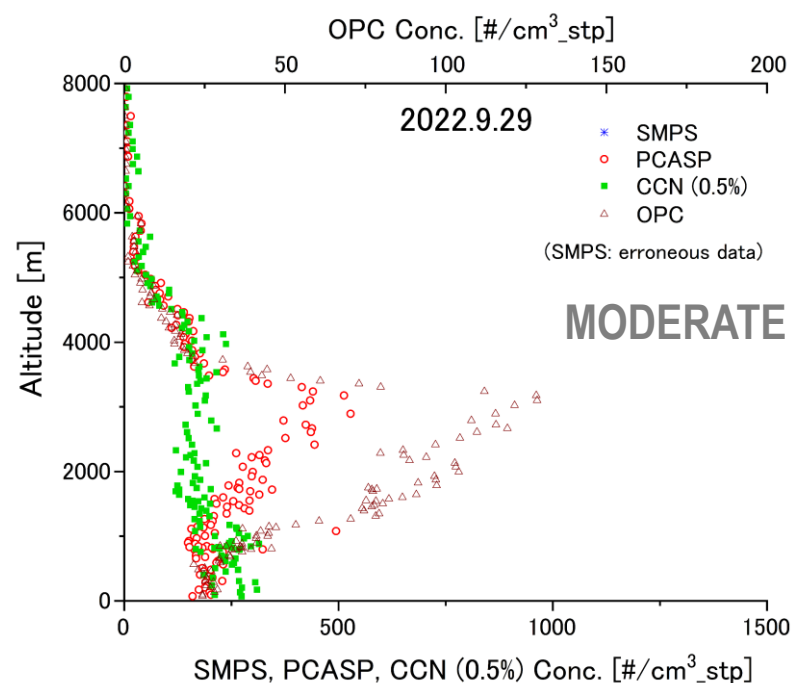
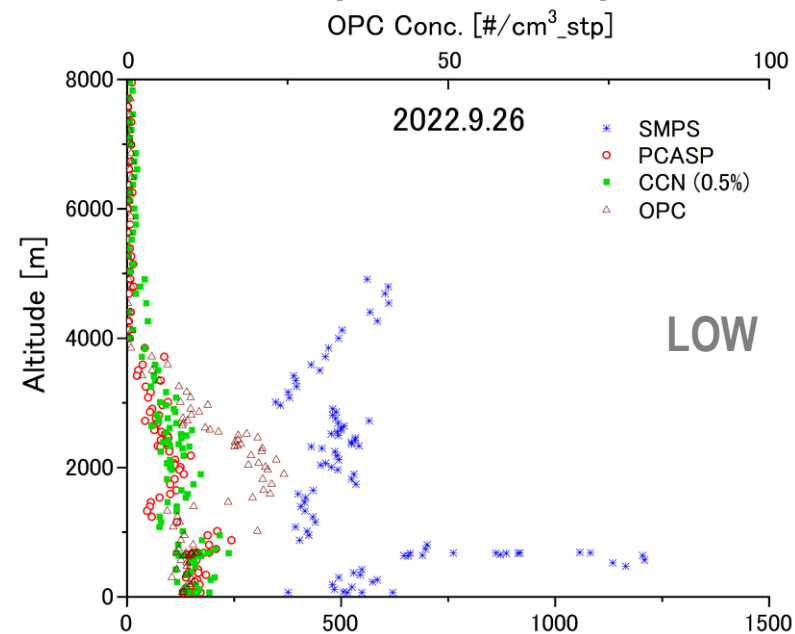
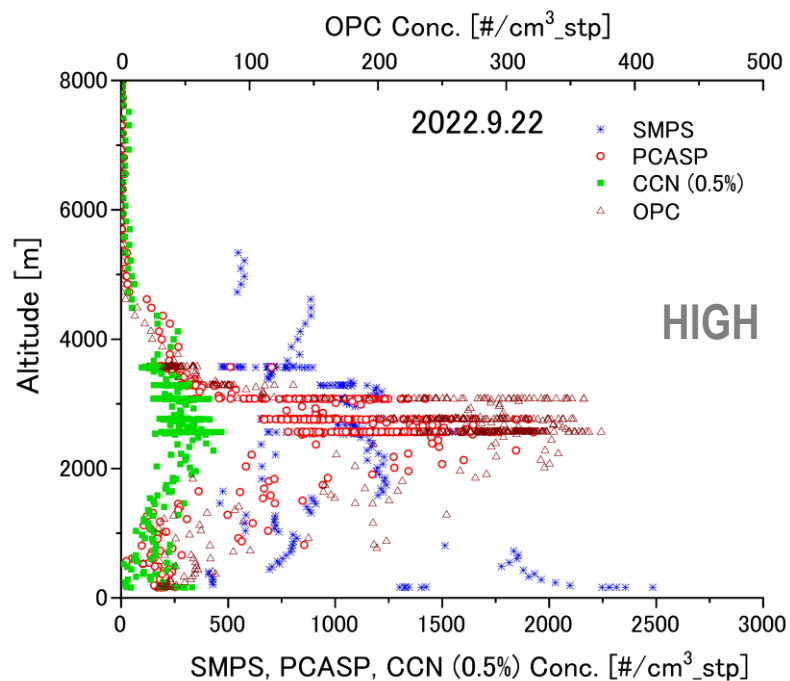


Vertical profiles of aerosol conc. (H < 8 km)

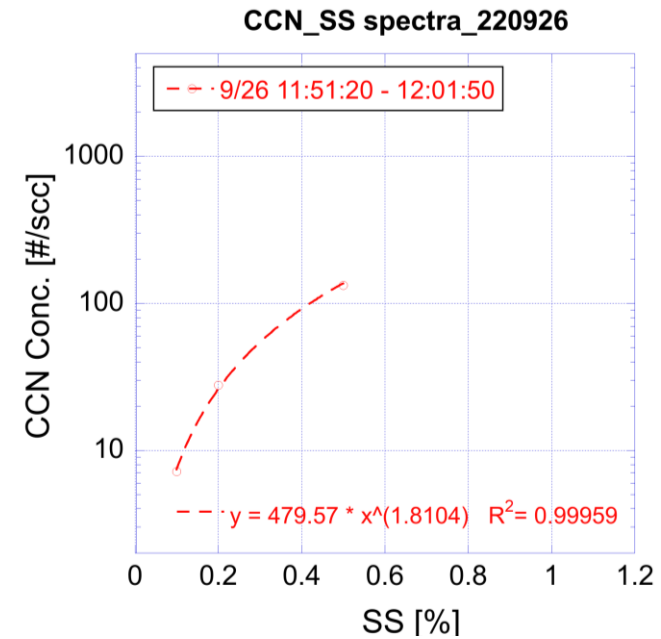
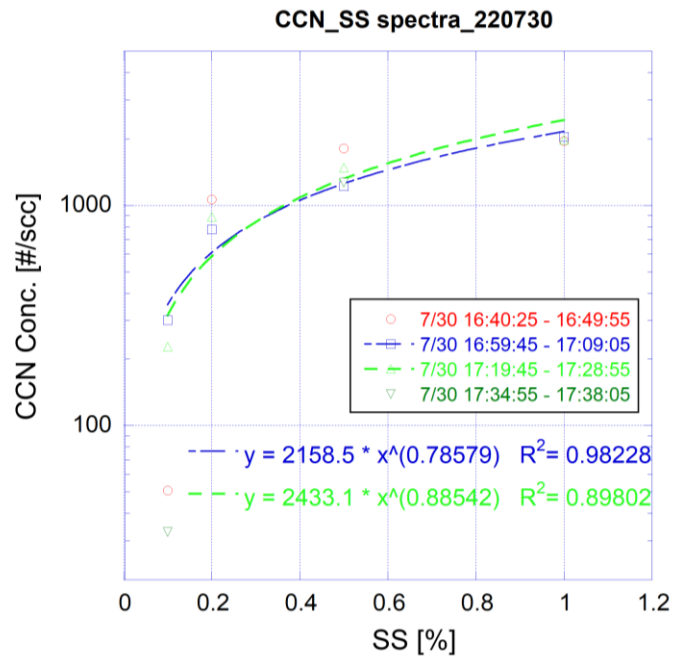
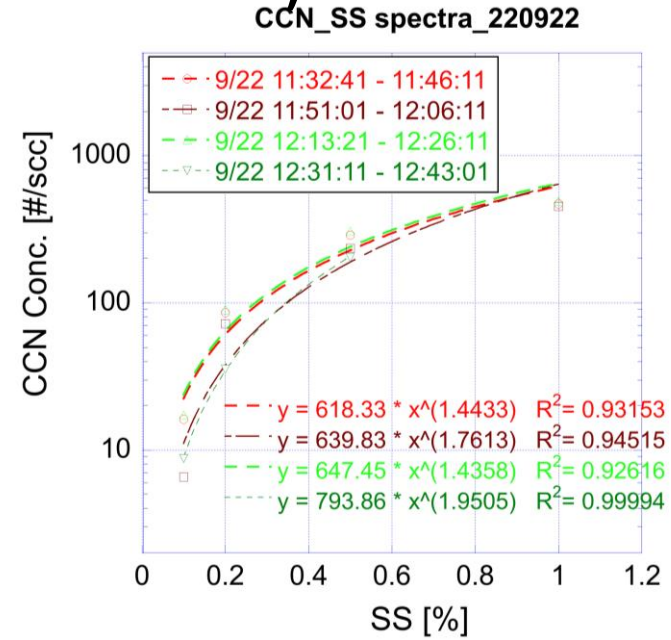
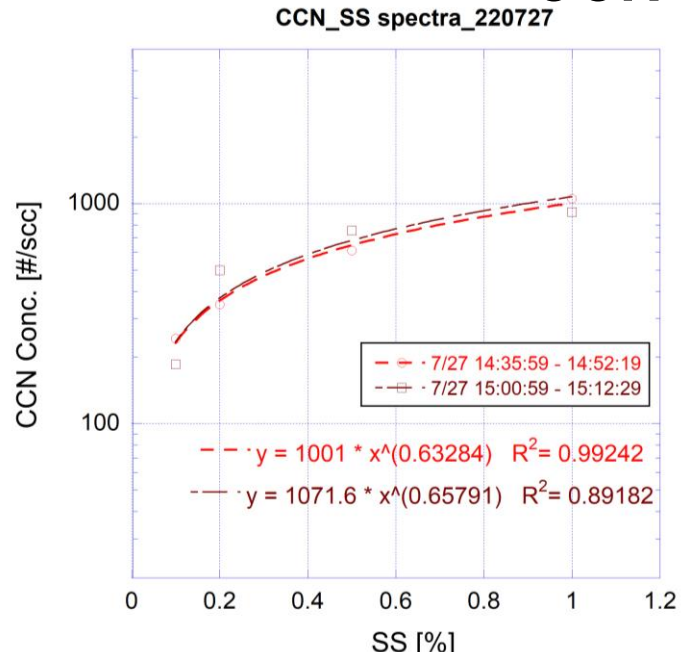


Vertical profiles of aerosol conc. (H < 8 km)

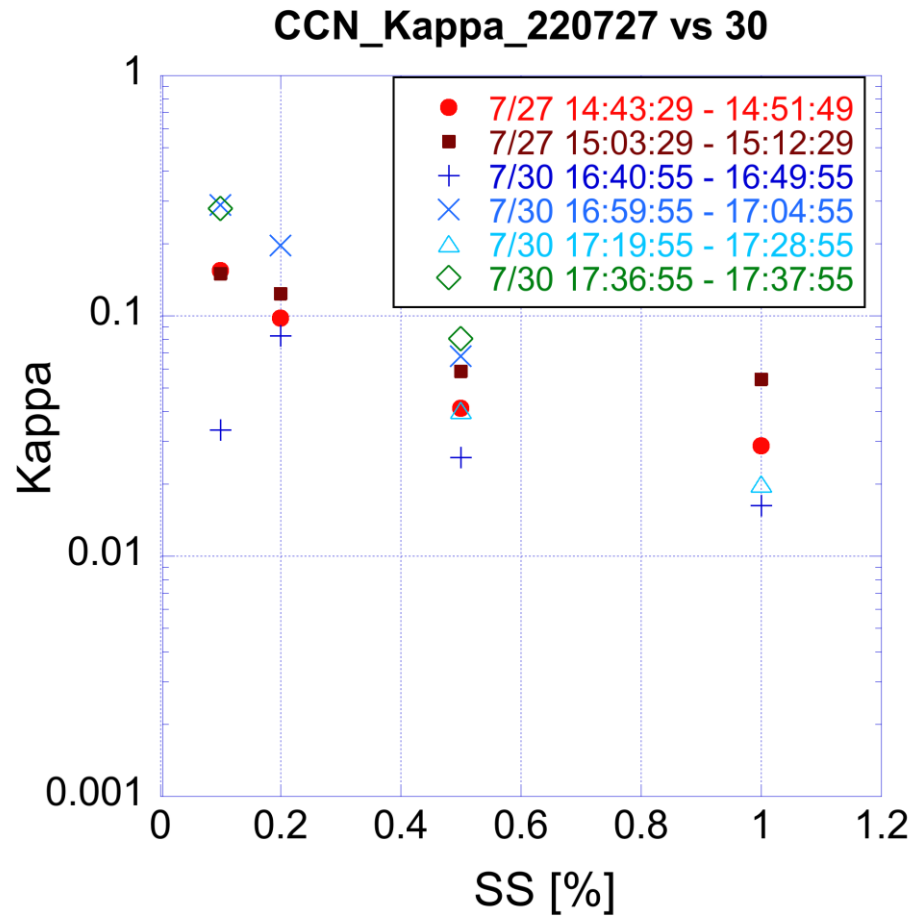
CPEX-CV



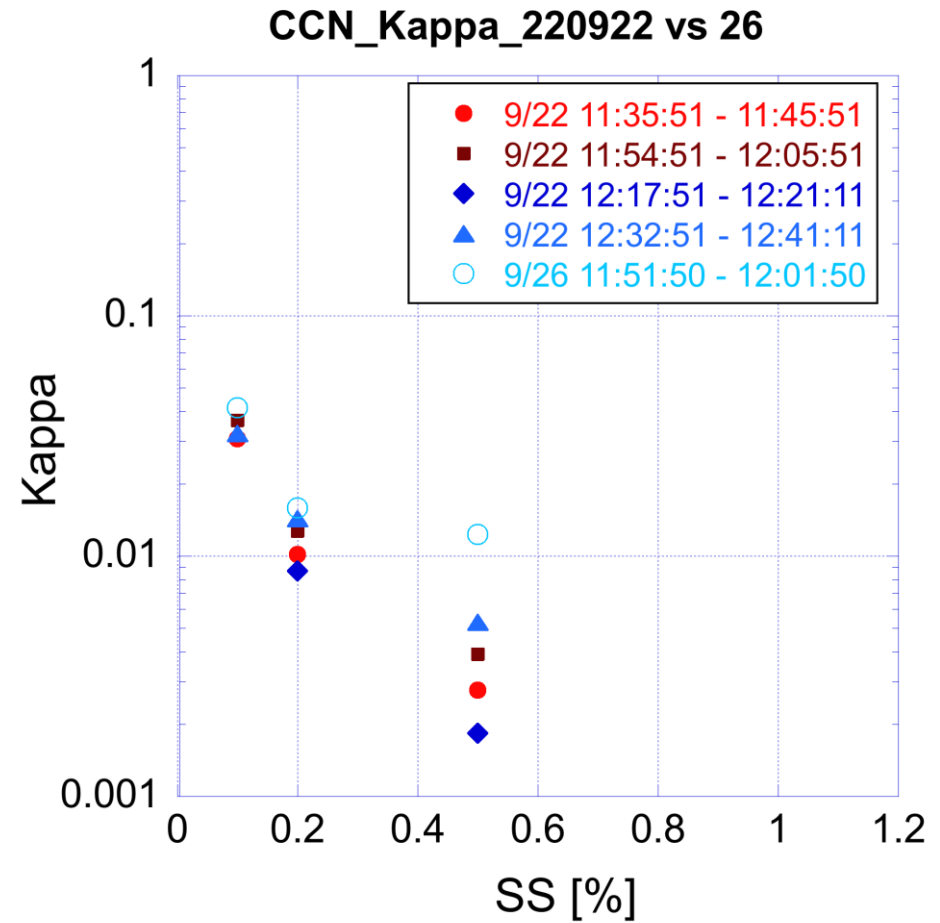
CCN SS spectra (at low levels)



Hygroscopicity (K) (at low levels)



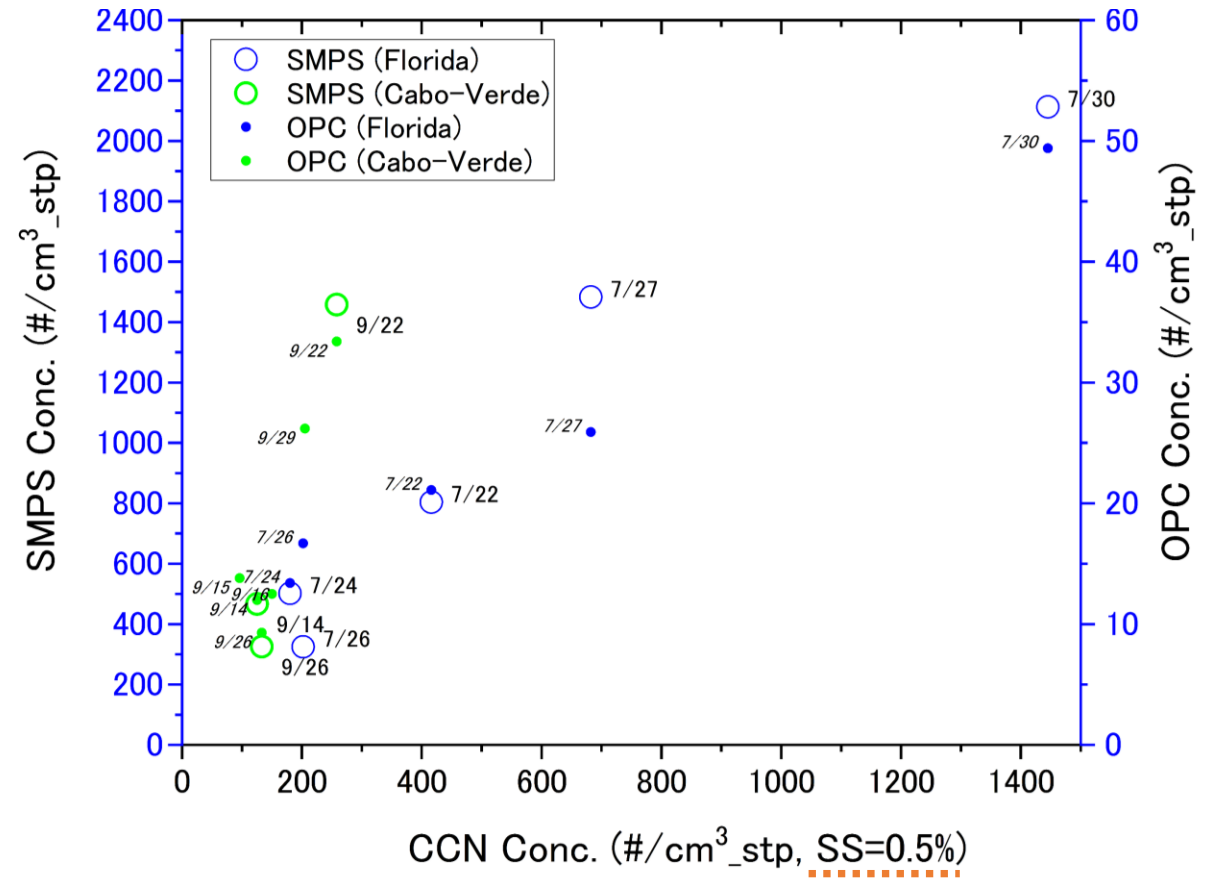
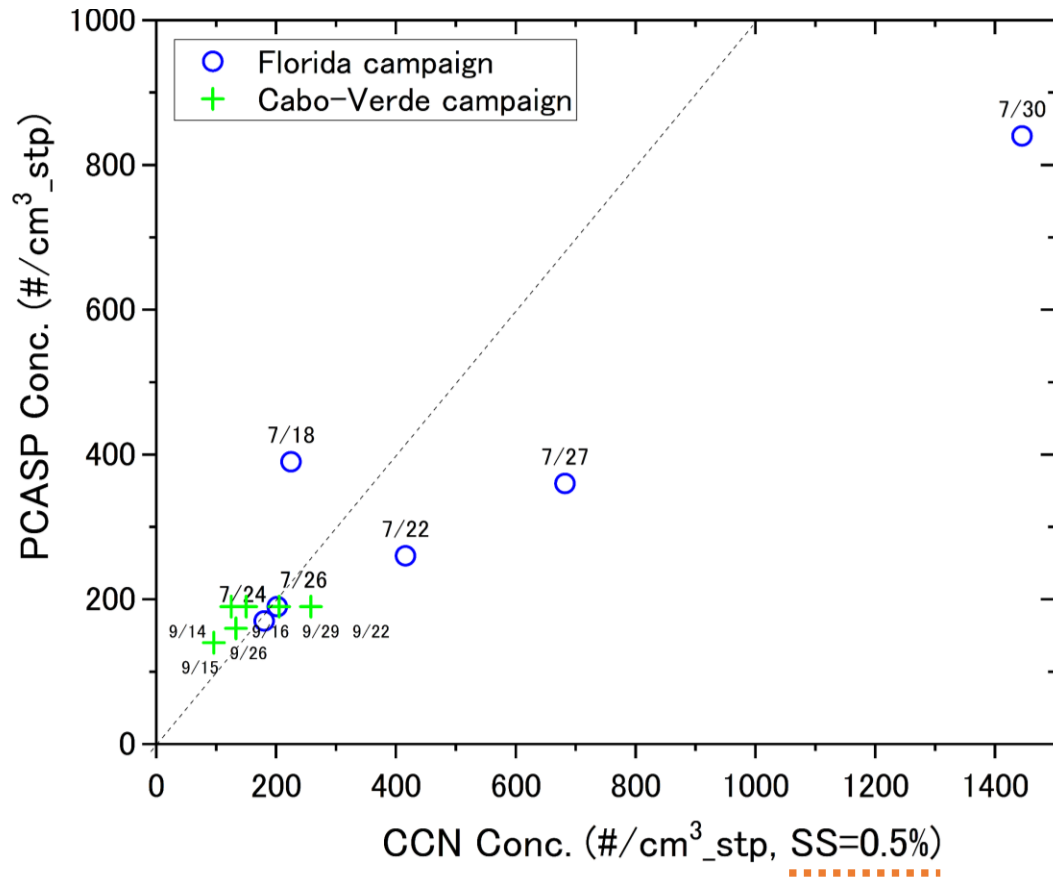
HIWC-2022



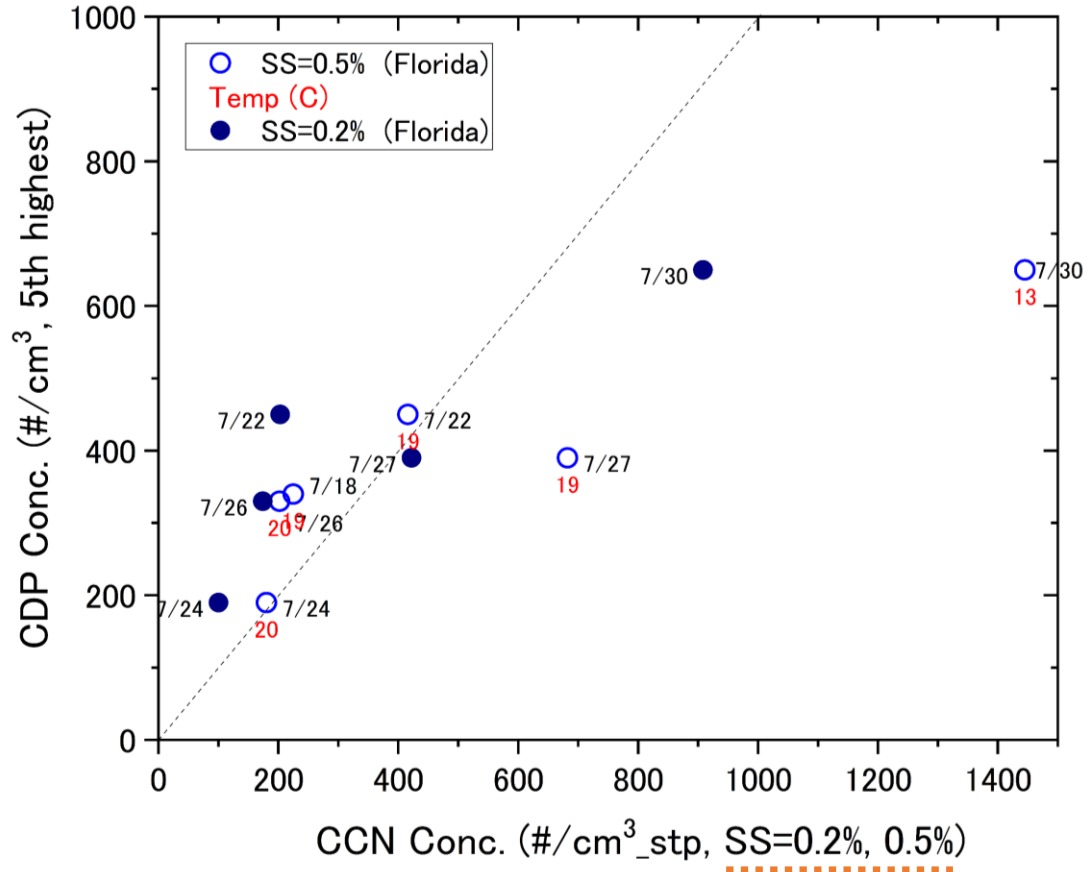
CPEX-CV

HIWC-2022
CPEX-CV

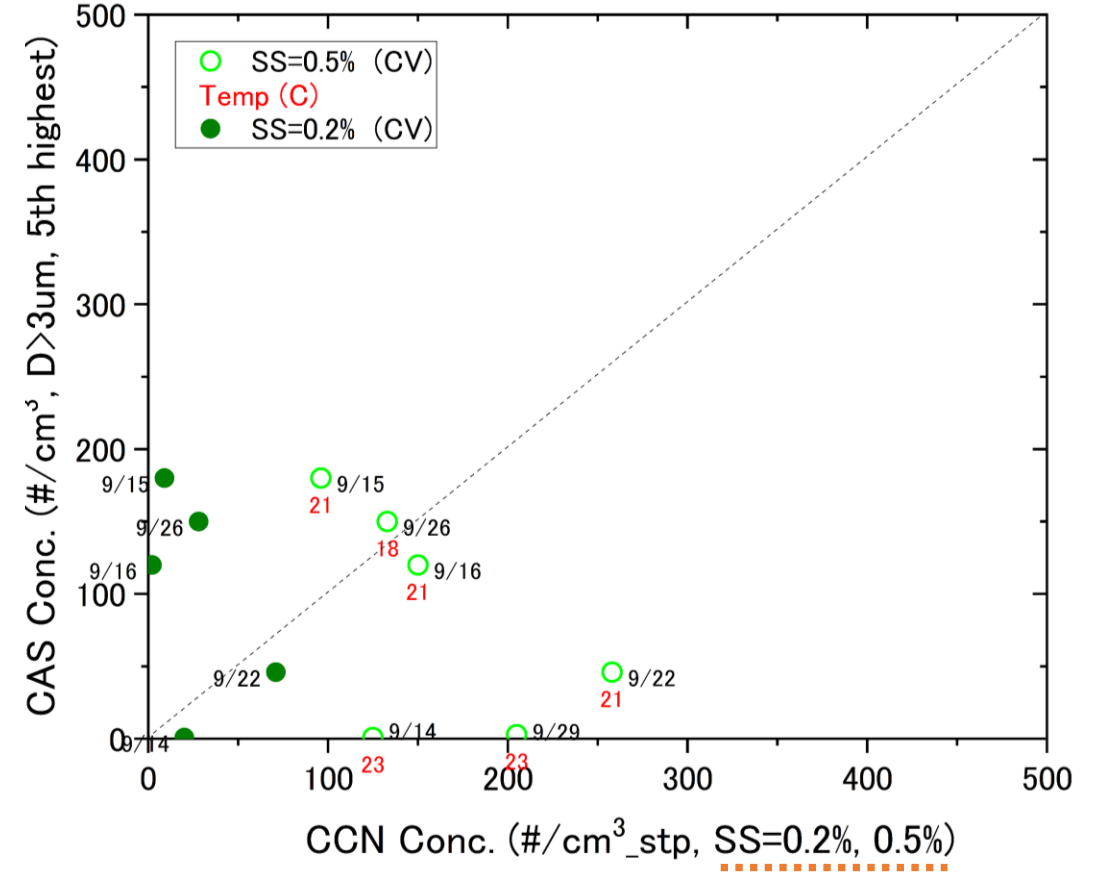
CCN vs PCASP or SMPS (at low levels, average)



CCN vs CDP or CAS (5th highest)



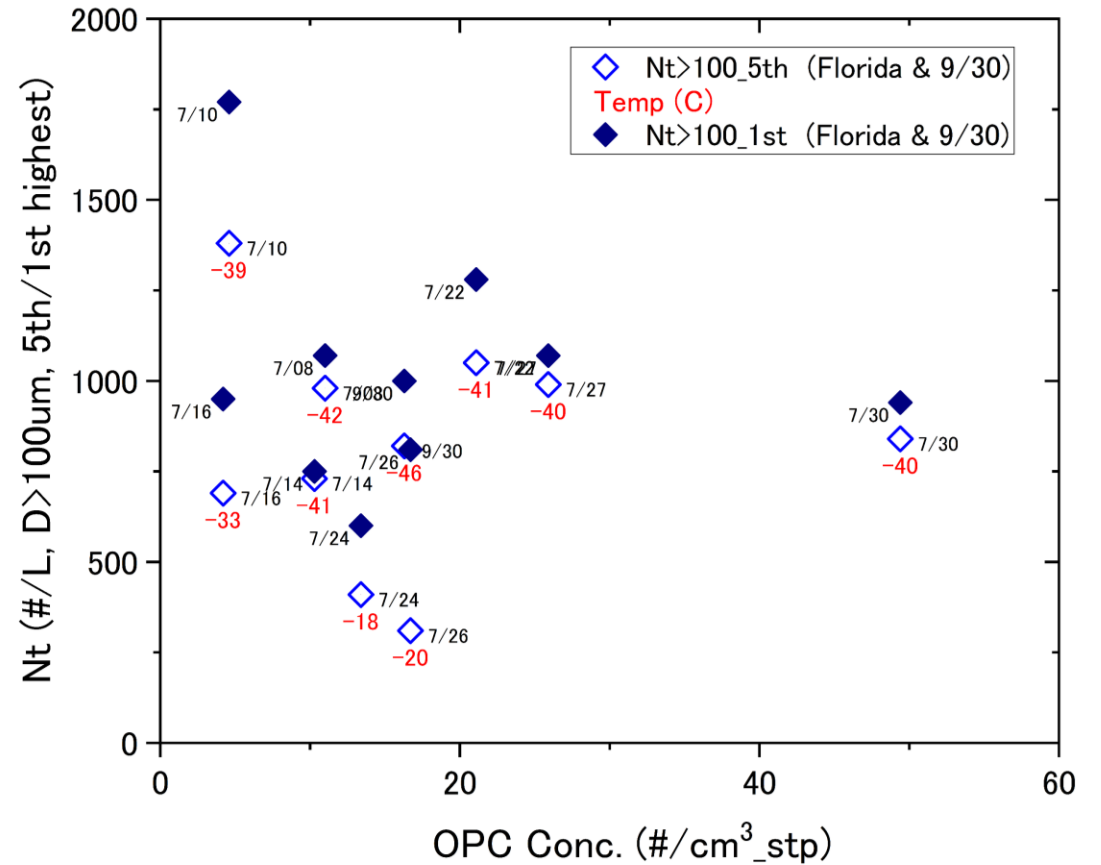
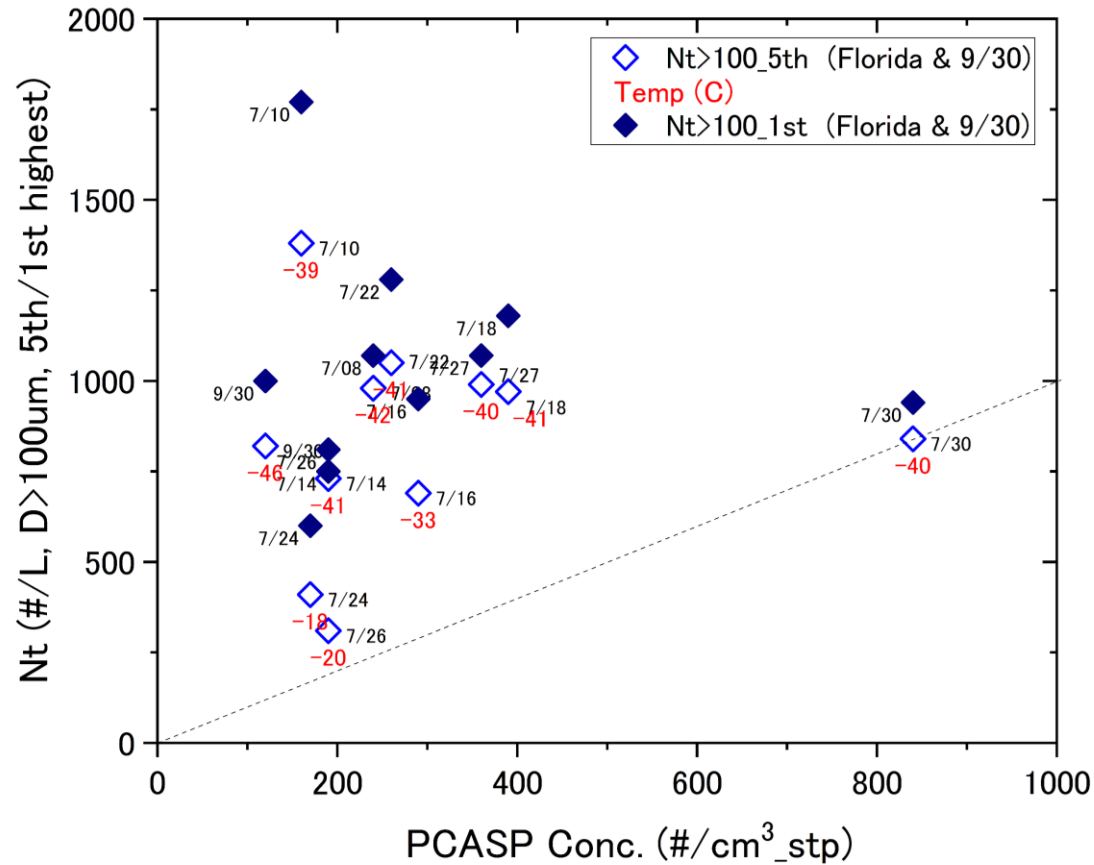
HIWC-2022



CPEX-CV

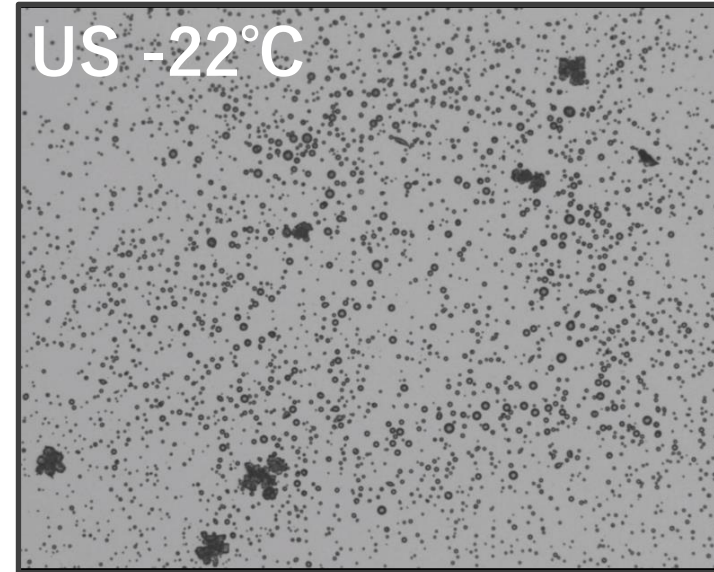
HIWC-2022, 9/30

PCASP or OPC vs 2DS+PIP (max.) (CIP for 9/30)

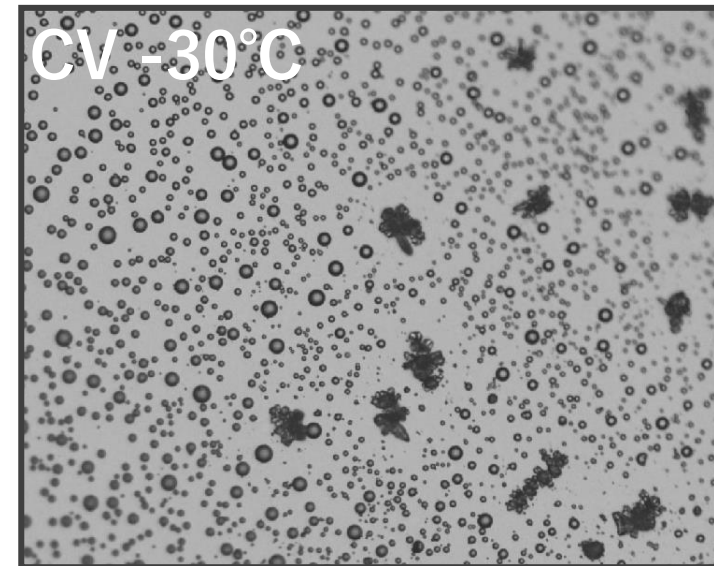


HIWC-2022

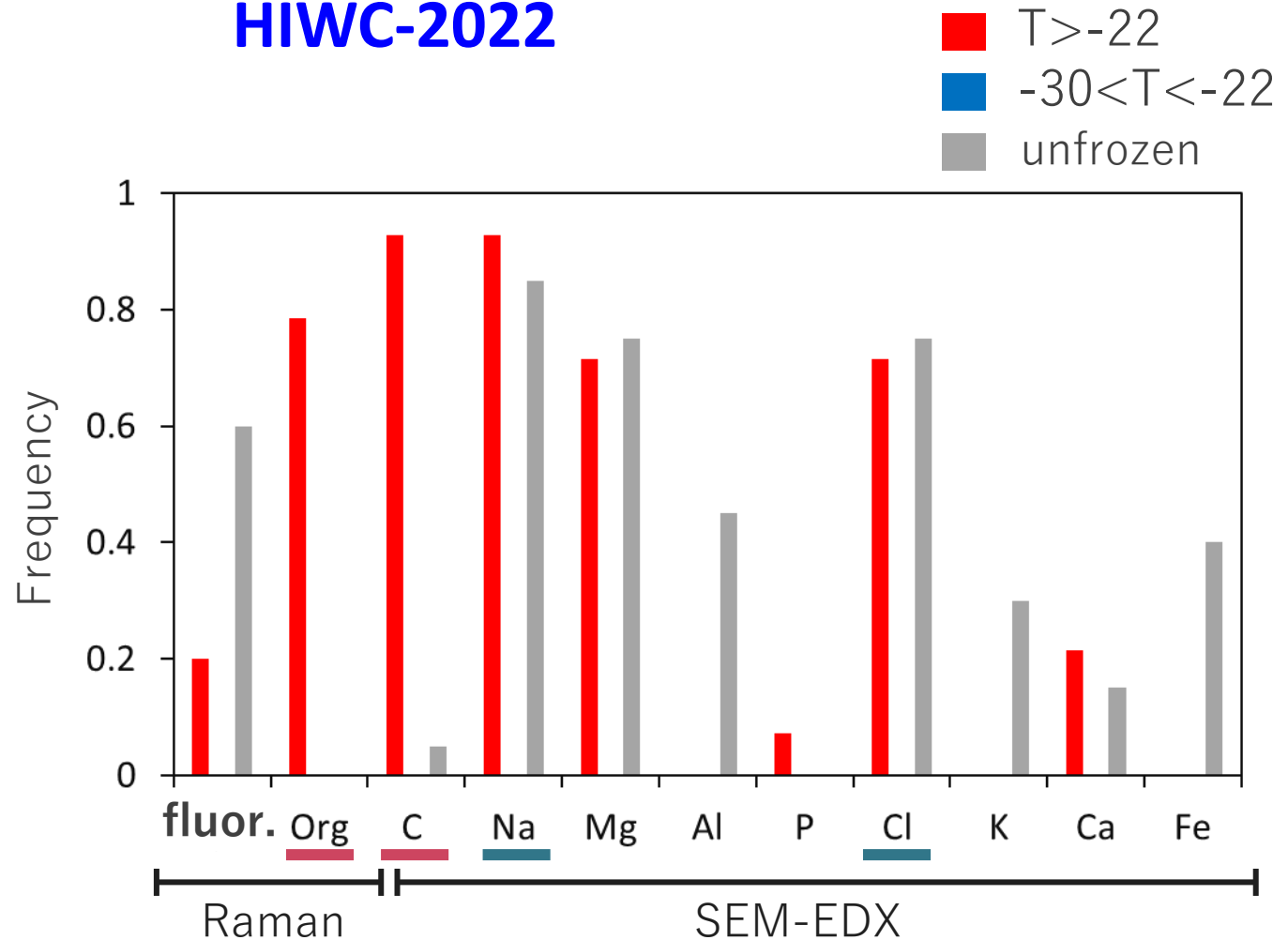
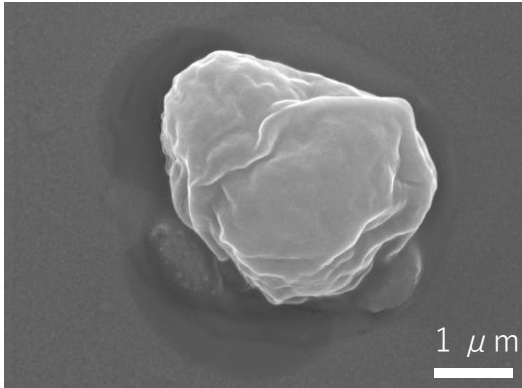
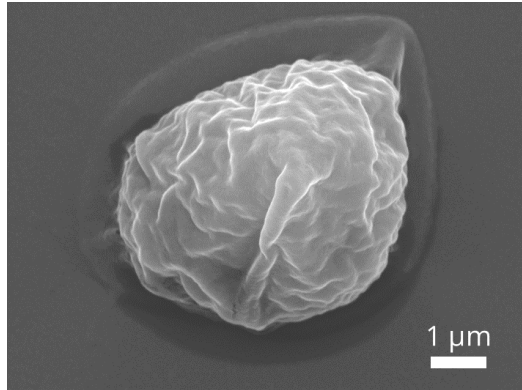
- Total [#] : 46693
- highest T : -19.2°C
- INP ($-30 < T < -22$) [#] : 42
- INP ($T > -22$) [#] : 15

**CPEX-CV**

- Total (#) : 27892
- highest T : -22.4°C
- INP ($-30 < T < -22$) [#] : 116
- INP ($T > -22$) [#] : 0

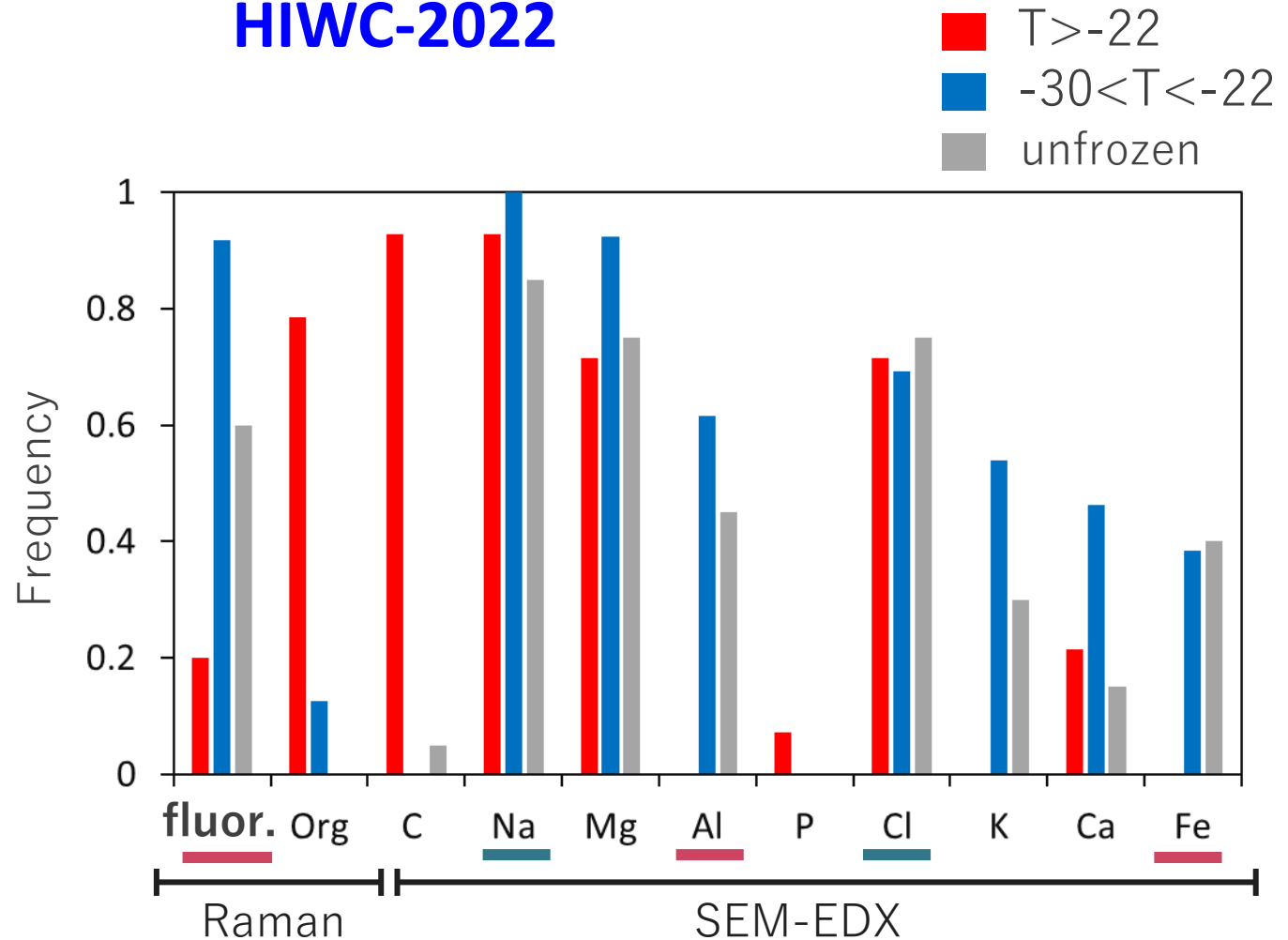
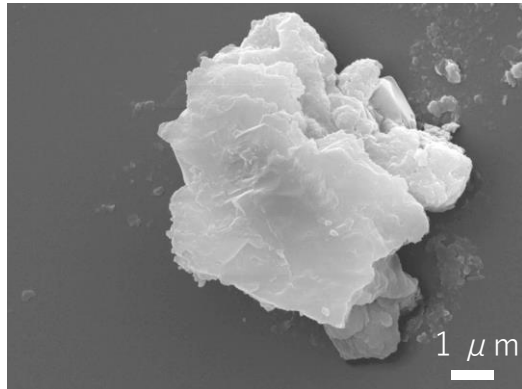
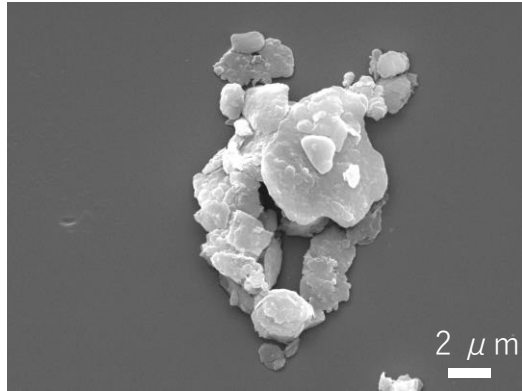


HIWC-2022



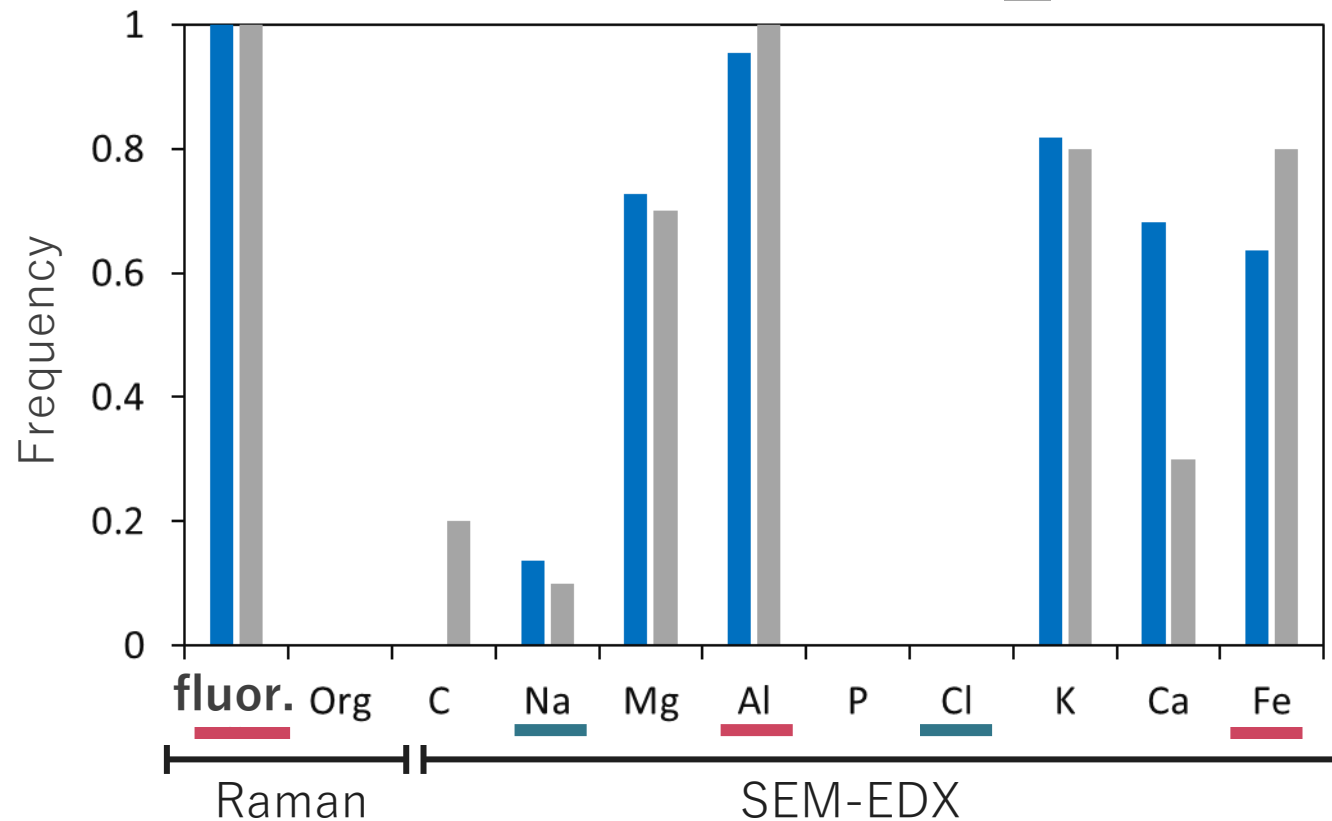
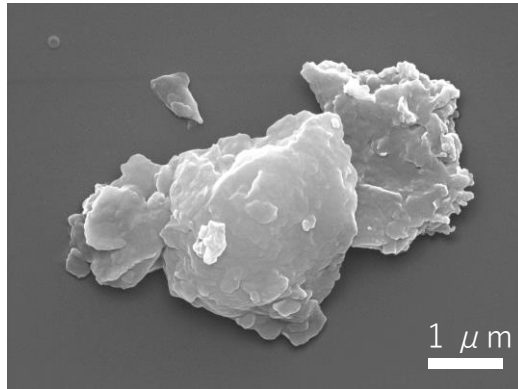
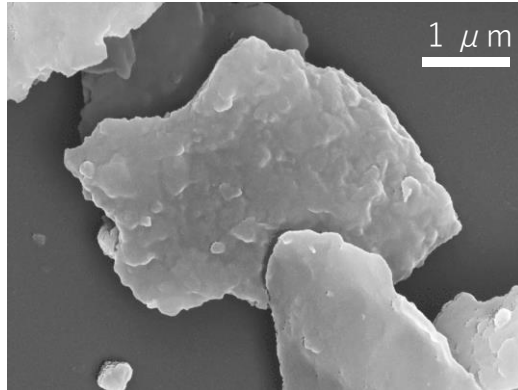
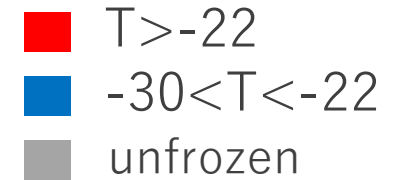
- ellipsoid shape, different from sea salt or mineral dust
- C-H band and/or C, which indicates organic substances
- bio-aerosol internally mixed with sea salt, which may cause higher activated T.

HIWC-2022



- non-spherical shape with asperity
- clay mineral feature: fluorescence, mineral particle feature: Al, Fe
- mineral dust internally mixed with sea salt

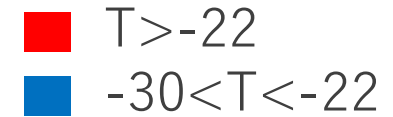
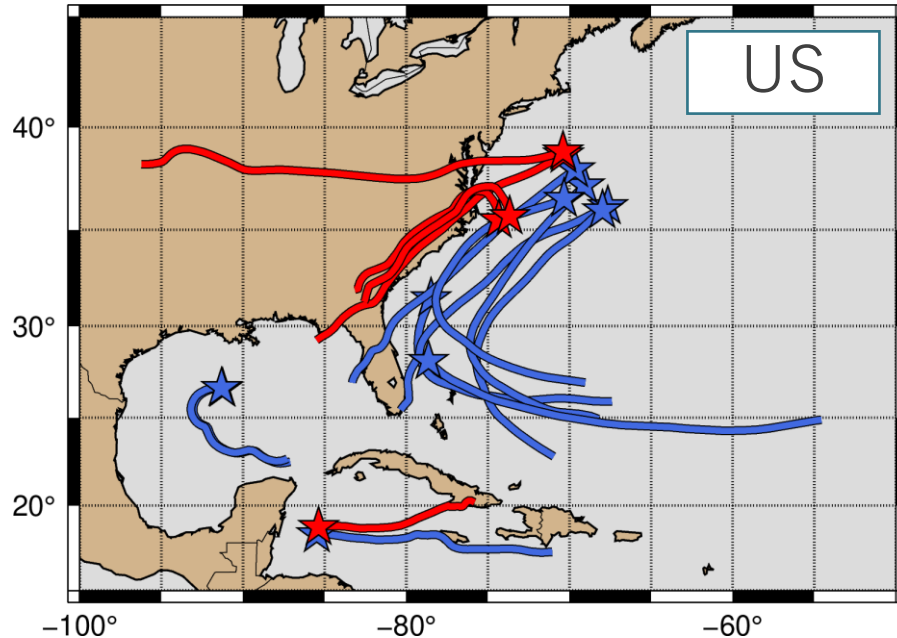
CPEX-CV



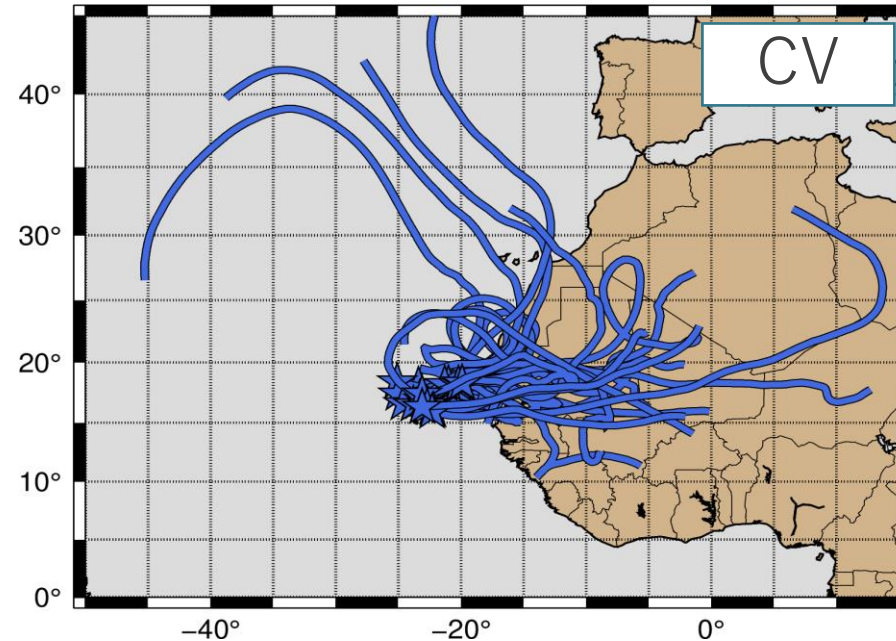
- non-spherical shape with asperity
- clay mineral feature: fluorescence, mineral particle feature: Al, Fe
- mineral dust externally mixed with others

HYSPLIT

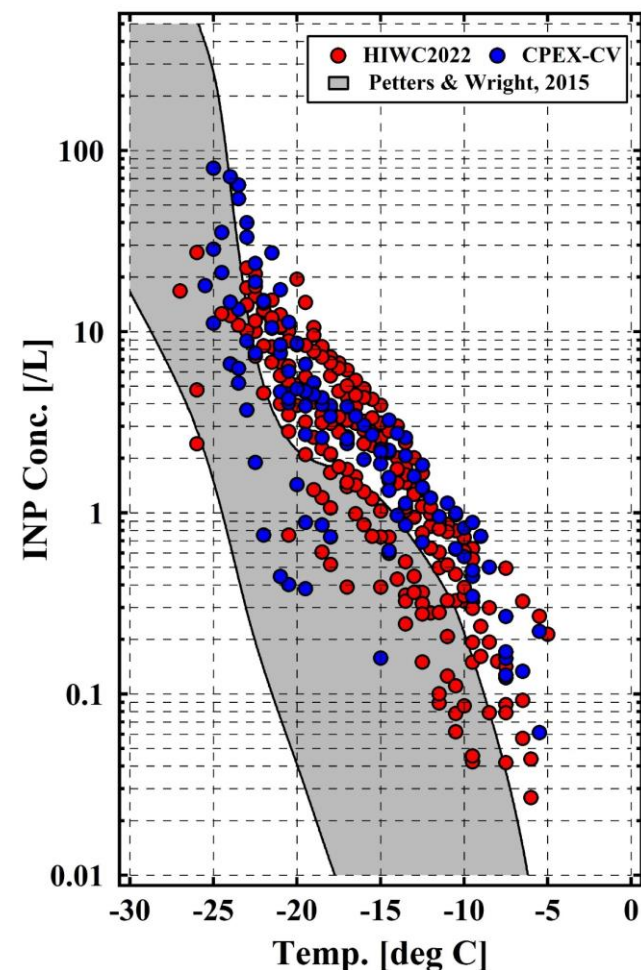
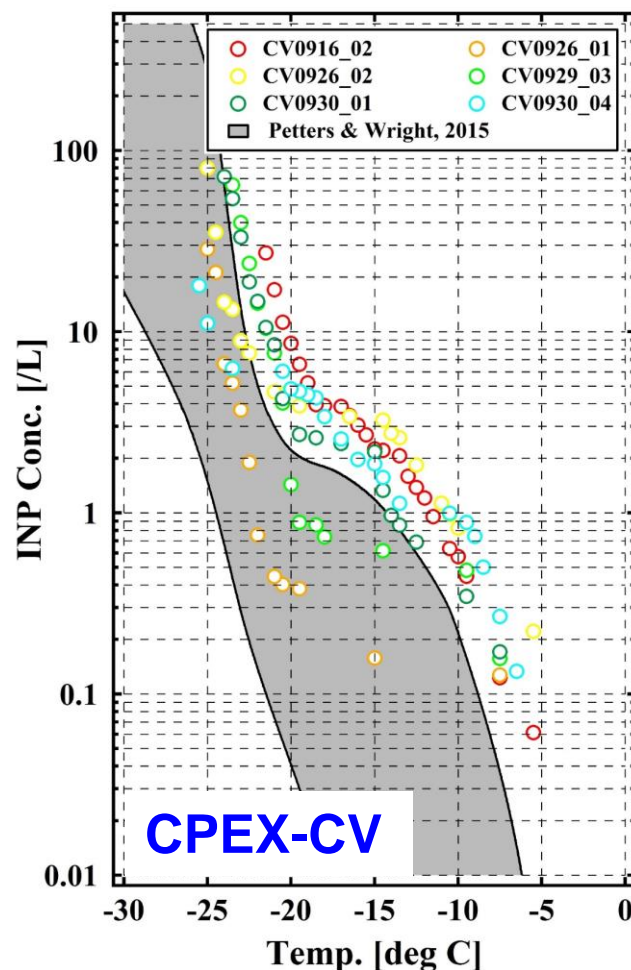
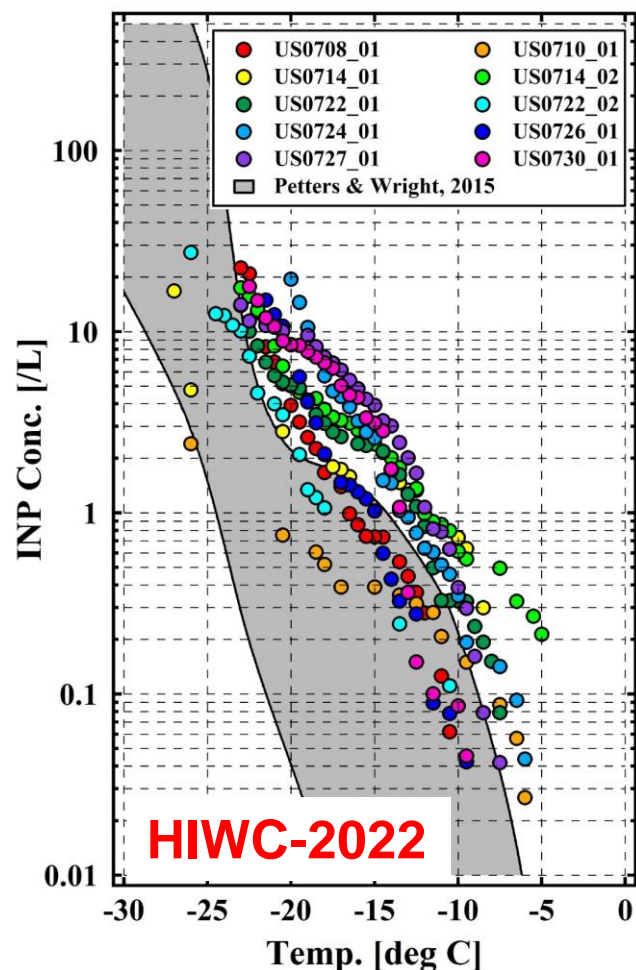
HIWC-2022



CPEX-CV

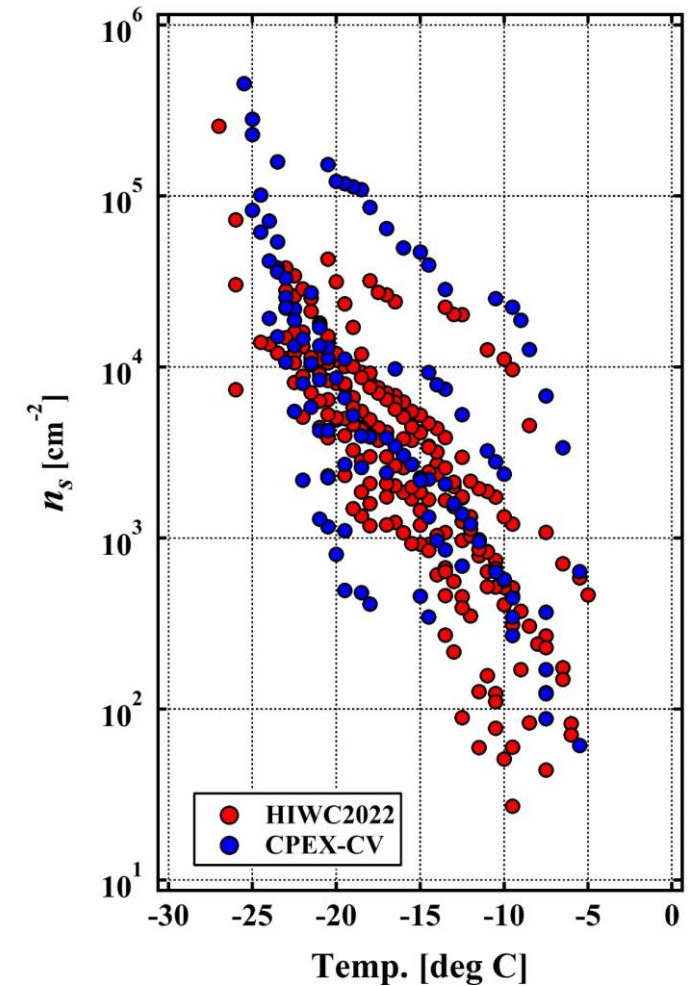
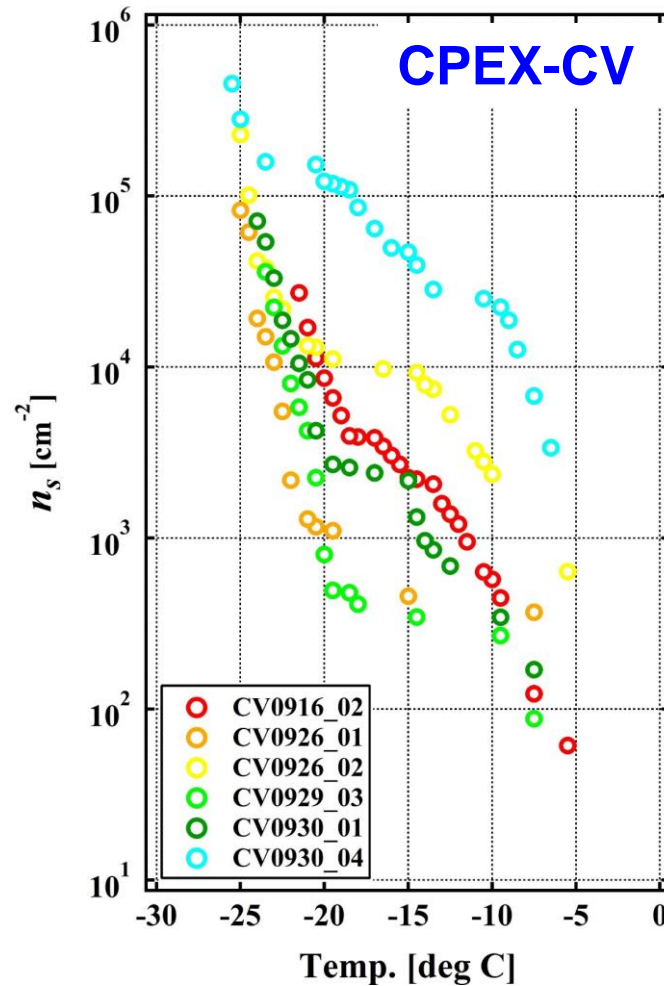
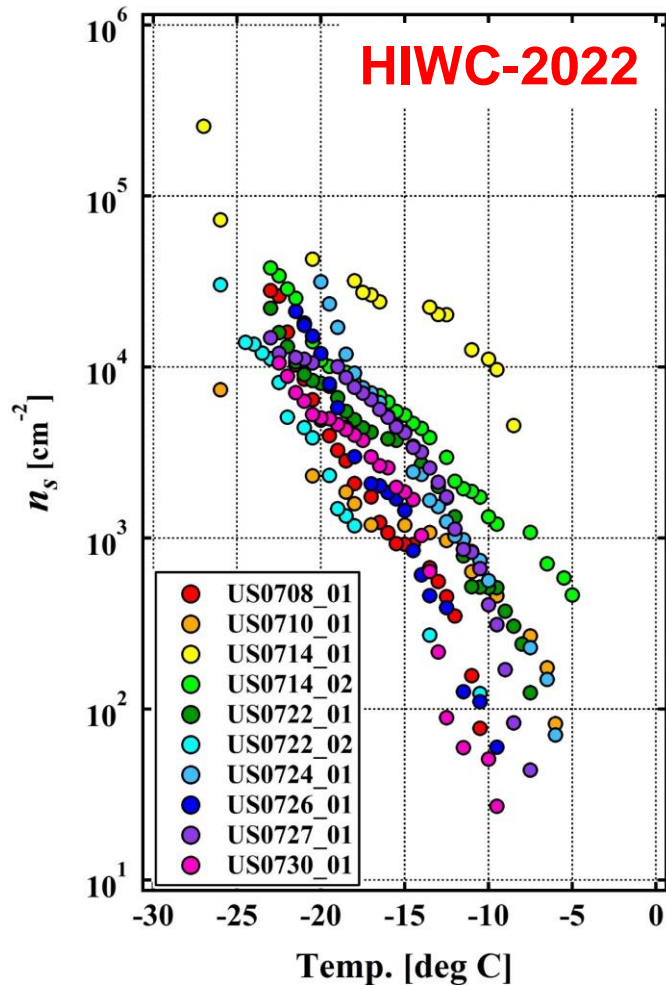


- bio-aerosol originated from the land, which contributed to freeze at higher T (US)
- externally mixed mineral dust originated from the Sahara desert (CV)



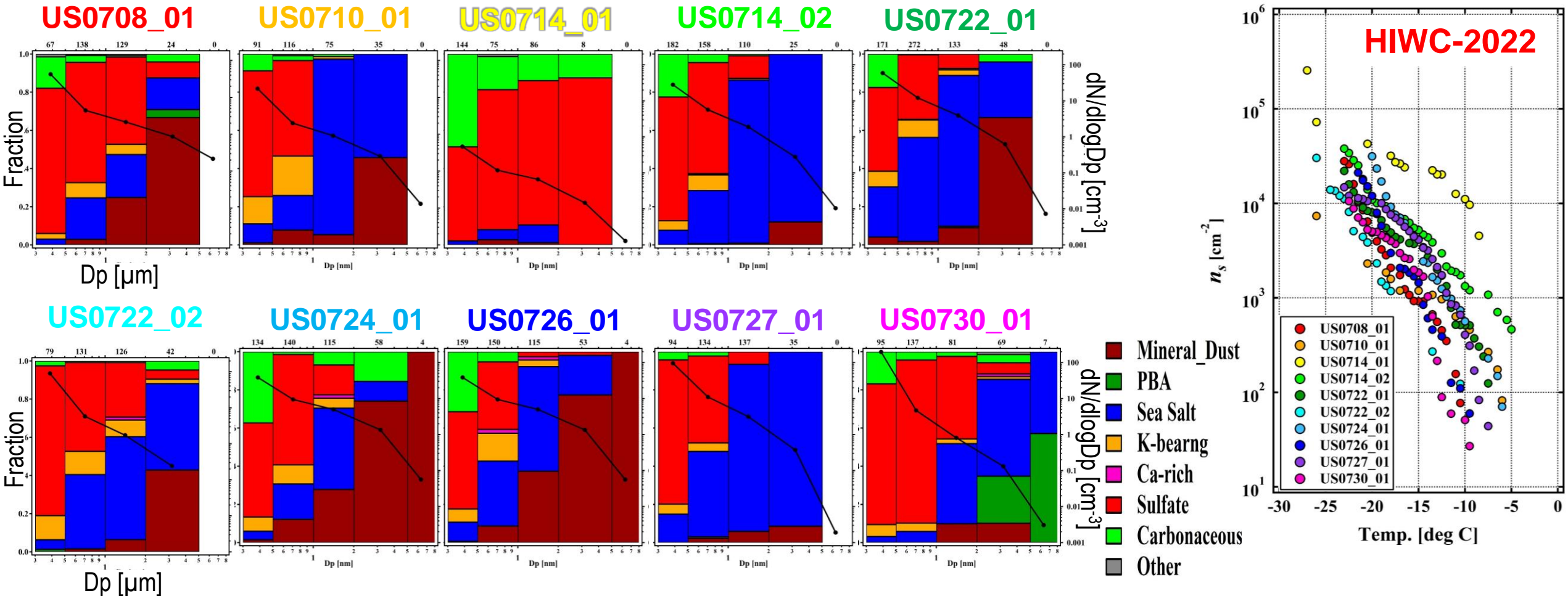
- comparable INP conc. to previous studies (various locations) (Kanji et al., 2017, Price et al., 2018)
- 1 ~ 2 order range in any T in both campaigns
- similar INP conc. between two campaigns, despite of different sampling locations and heights

Ice Nucleation Active Site (INAS) Densities



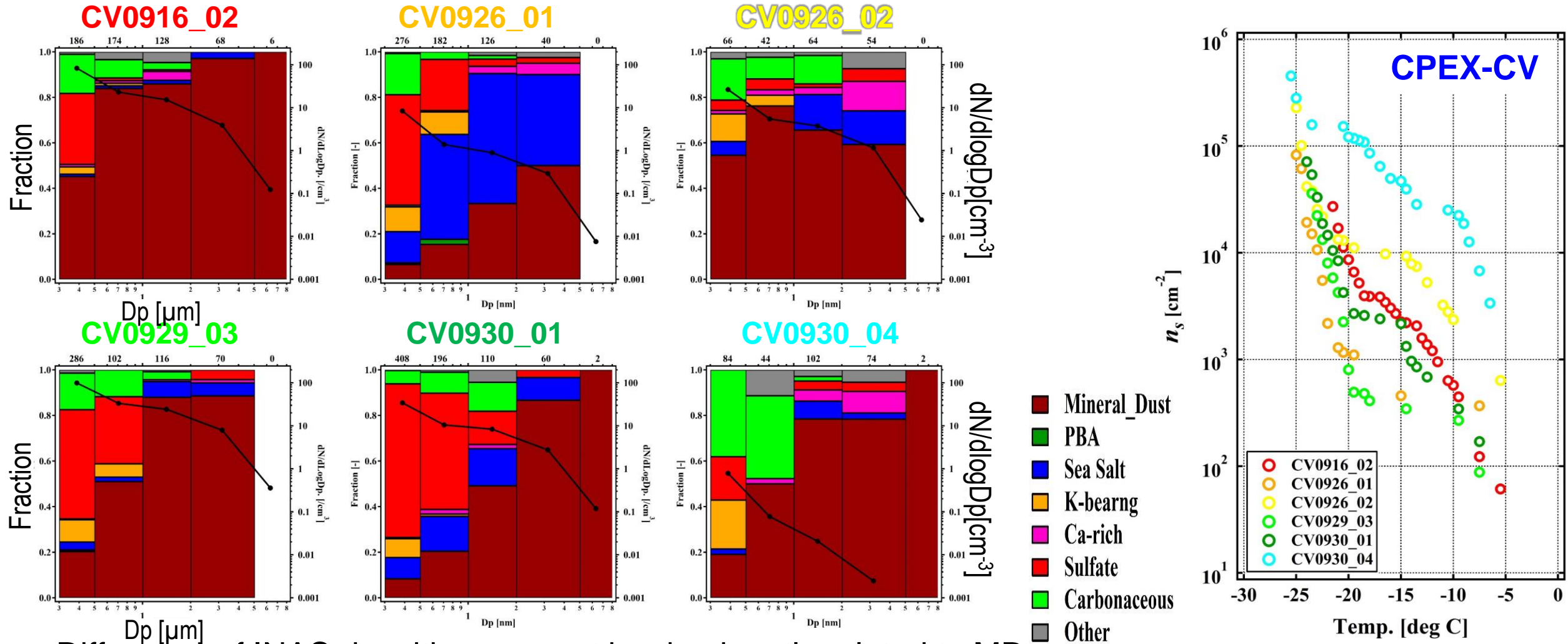
- INAS was calculated based on size distributions over all ranges (SMPS+OPC)
- no significant differences between two campaigns
- rapid increase at $T < -20^{\circ}\text{C}$ in CPEX-CV

INAS Densities vs Particle Types



- Difference of INAS densities may not be related to MD and/or biogenic aerosols.
- INAS variations among cases were not clearly understood, although various types were classified.
 - Partly because contributions of INP surface areas to all areas may be small ?

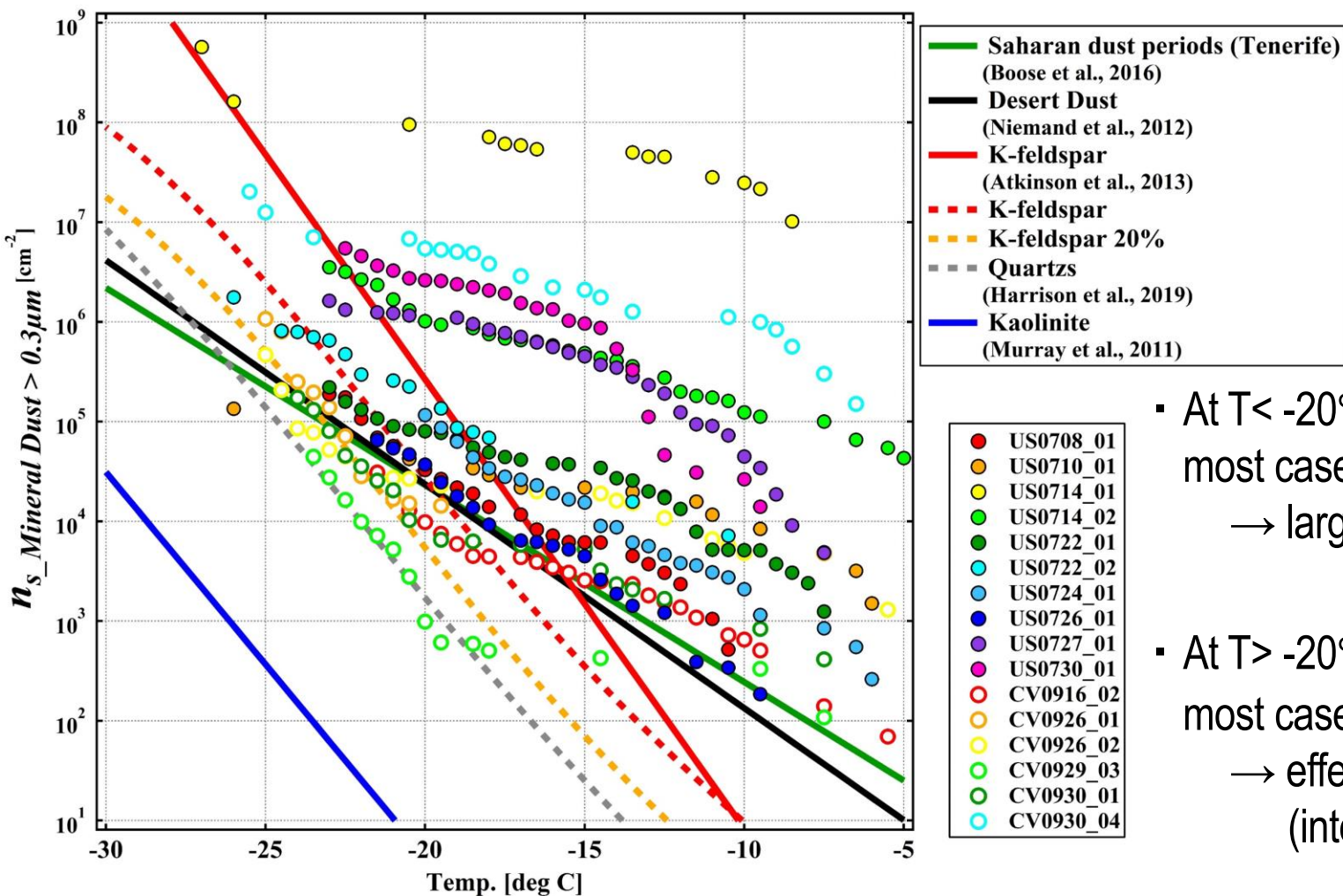
INAS Densities vs Particle types



- Difference of INAS densities may not be dominantly related to MD.
- In CPEX-CV, INAS variations among cases were not clearly understood, although most type was MD.
 - Partly because contributions of INP surface areas to all areas may be small ?

Contributions of Mineral Dust

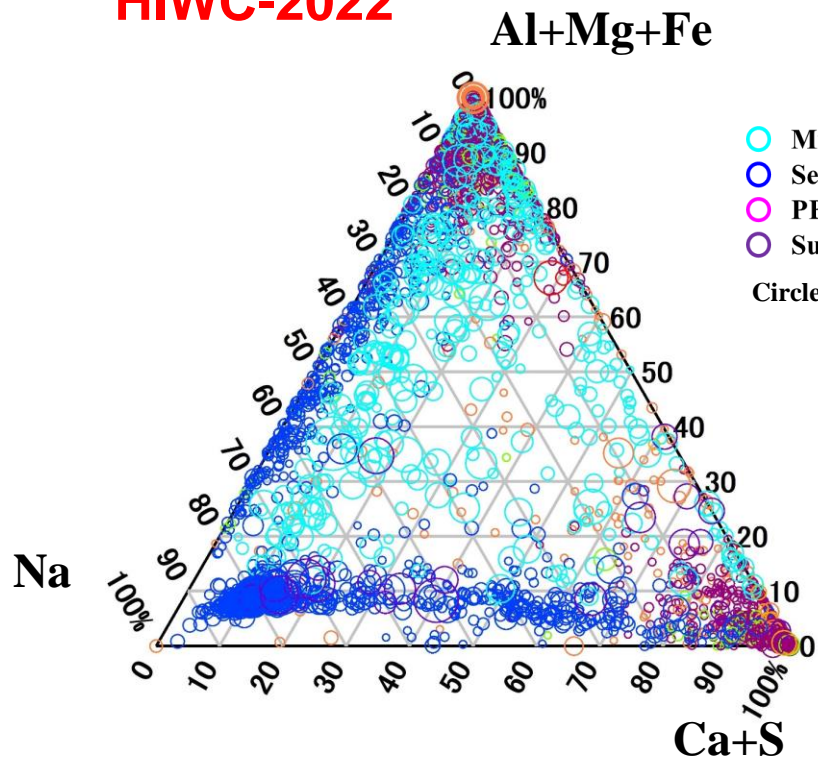
If all INPs were mineral dust (MD), INAS curves converged to those of standard dust particle ...
 (vertical axis: INAS from the aerosols classified as MD and larger than 0.3 μ m)



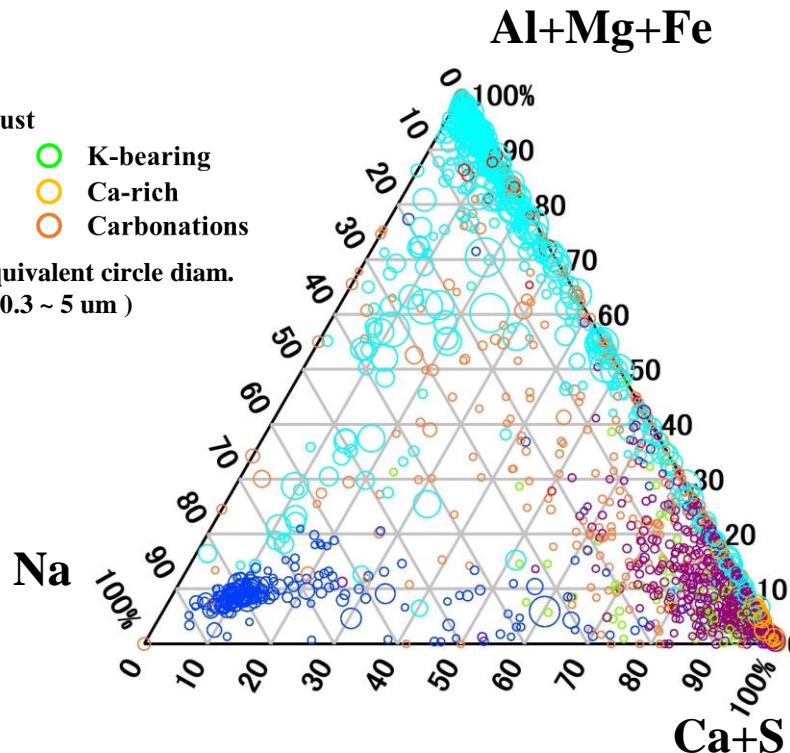
- At $T < -20^{\circ}\text{C}$, except for some cases, most cases converged to INAS for standard MD \rightarrow large contributions of MD
- At $T > -20^{\circ}\text{C}$, regardless of primary biogenic aerosols (US0730_1), most cases deviated from INAS for standard MD \rightarrow effects of other categories than MD? (internally mixed biogenic compounds?)

Internally Mixed Particles

HIWC-2022

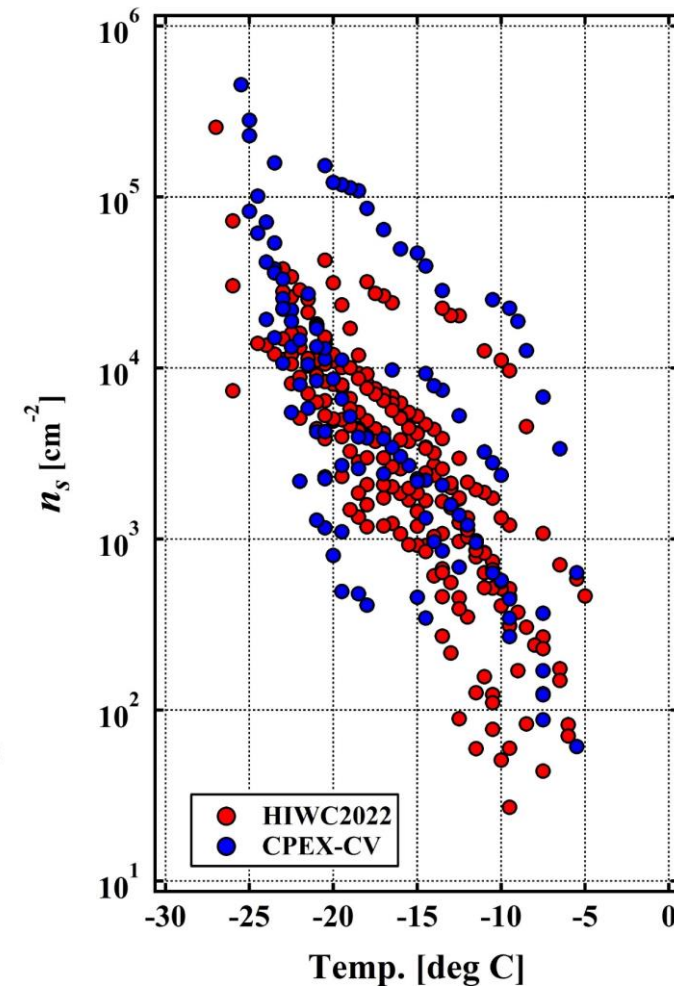


CPEX-CV



Ternary diagram for wt % ratios

- Mineral Dust
 - Sea Salt
 - PBA
 - Sulfate
 - K-bearing
 - Ca-rich
 - Carbonations
- Circle Size: equivalent circle diam. (0.3 ~ 5 μm)



In **HIWC-2022**, contrast to CPEX-CV,

- Mineral dust (MD), without detection of Fe or internally mixed with sea salt, was characteristic.
- Contributions of MD may be underestimated, which caused to weaken the relations between particle classification and INAS.

Summary and future work

(CCN and aerosol)

- Aerosol number concs. were highly variable in both campaigns in terms of vertical and horizontal distributions.
- CCN number concs., as well as CCN spectra, were well-correlated with aerosol loading in HIWC-2022, but not so correlated (mostly low CCN) in CPEX-CV.
- κ was higher at any SS in HIWC-2022 than in CPEX-CV. The values were small compared to typical continental case.

(INP #1)

- Bio-aerosol internally mixed with sea salt, which originated from the land, may cause high activated T in HIWC-2022.
- No particles activated at $T > -22^\circ\text{C}$ in CPEX-CV. Mineral dust internally mixed with sea salt, which originated from the Sahara desert, activated at $T < -22^\circ\text{C}$.

(INP #2)

- INP number concs. in both campaigns were similar and comparable to previous studies.
- INAS at $T < -20^\circ\text{C}$ may be explained through the dust parameterizations from previous studies.
- INAS at $T > -20^\circ\text{C}$ was difficult to explain or understand in context of the dust parameterizations.

(Future work)

- Size dependency on CCN and INP activations
- Difference between activated and non-activated aerosol, even in bio-aerosol category
- Evaluation of mineral dust particles internally mixed with other categories

Backup Slides

κ value of a given chemical composition

κ -Köhler theory

Petters and Kreidenweis, 2007

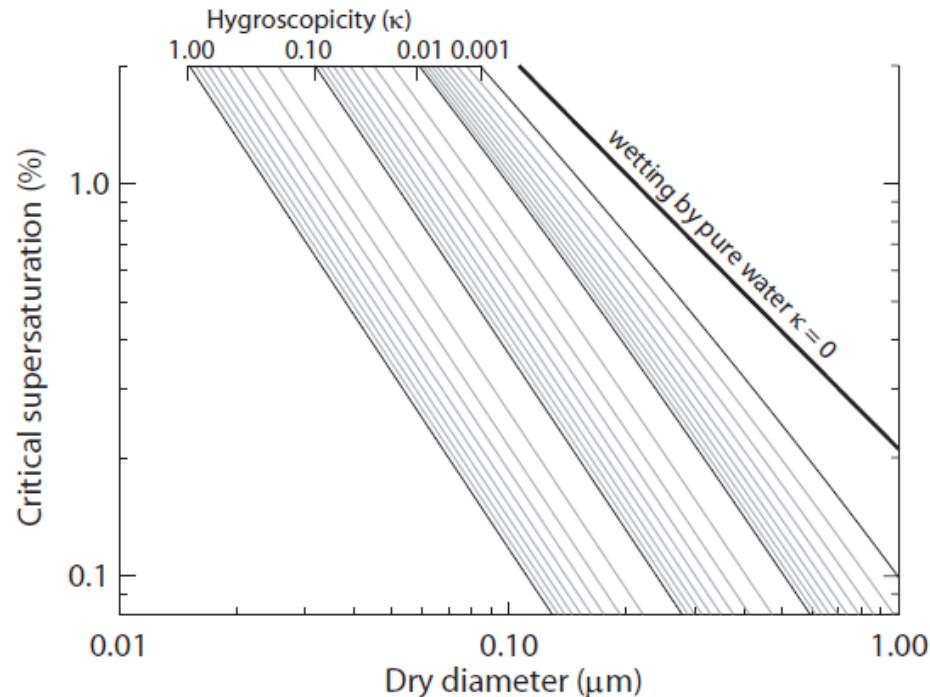
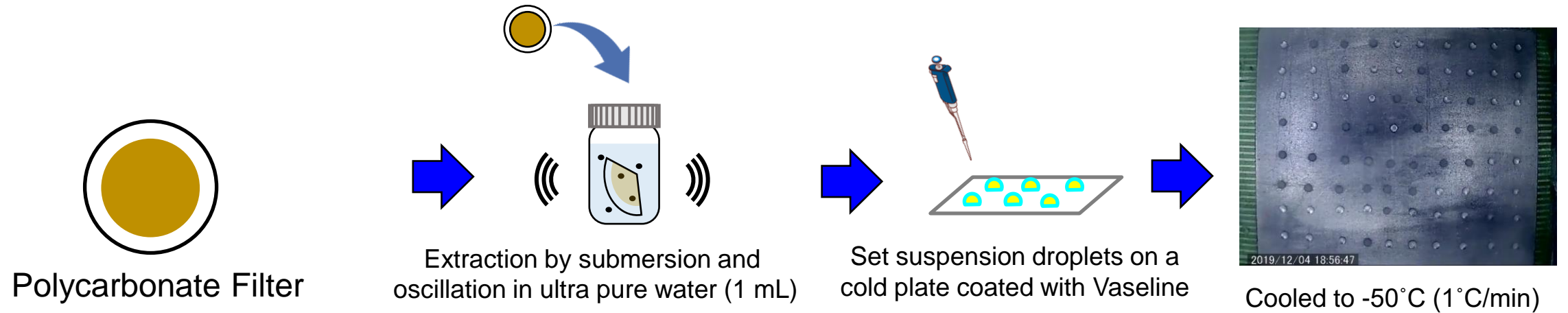


Fig. 1. Calculated critical supersaturation for $0 \leq \kappa \leq 1$ computed for $\sigma_{s/a} = 0.072 \text{ J m}^{-2}$ and $T = 298.15 \text{ K}$. The gray lines are linearly spaced intermediates.

Particle Type	κ
$(\text{NH}_4)_2\text{SO}_4$	0.61
NaCl	1.28
Arizona Test Dust	0.025
Sahara Dust	0.054

small $\kappa \Rightarrow$ growth similar to pure water
large $\kappa \Rightarrow$ larger solute effect
typical value κ (ambient air) : 0.1-0.9

➤ Typical IN assay by cold plate



This study !!

Method & Analysis (INP) #2

➤ Droplet Freezing Assay on Filter

